DIGITALCOMMONS
—@WAYNESTATE—

Wayne State University

Wayne State University Dissertations

1-1-2016

Essays On Oil Price Volatility And Irreversible Investment

Daniel Joseph Pastor
Wayne State University,

Follow this and additional works at: https://digitalcommons.wayne.edu/oa_dissertations

Part of the Economics Commons, and the Oil, Gas, and Energy Commons

Recommended Citation

ESSAYS ON OIL PRICE VOLATILITY AND IRREVERSIBLE INVESTMENT

by

DANIEL J. PASTOR

DISSERTATION

Submitted to the Graduate School

of Wayne State University,

Detroit, Michigan

in partial fulfillment of the requirements

for the degree of

DOCTOR OF PHILOSOPHY

2016

MAJOR: ECONOMICS

Approved By:

_____

Advisor   Date

_____

_____

_____

DEDICATION

This work is dedicated to all my family and friends who have shown support for me in this endeavor. Without your support, this would not have been possible.

Thank you for everything.

TABLE OF CONTENTS

LIST OF TABLES

LIST OF FIGURES

CHAPTER 1: FORECASTING CRUDE OIL PRICE VOLATILITY[1]

INTRODUCTION

Large variations in the price of crude oil have been observed during the past decade. The price for West Texas Intermediate (WTI) reached a maximum of \$145.31 on July 3, 2008, possibly a consequence of geopolitical tensions over Iranian missile tests. It then fell sharply to \$91.49 on September 16, 2008 in the midst of the financial crisis, and fluctuated around \$40 by the end of the year. Such large swings in the crude oil price, in conjunction with a widespread consensus that large fluctuations in the price of oil are detrimental for economic activity, has bolstered a line of research into how to improve oil price forecasts.[2] This direction of research has provided important insights into the usefulness of macroeconomic aggregates, asset prices, and futures prices in forecasting the spot price of oil, as well as into the extent to which the real and the nominal price of oil are predictable.

Despite this rich and growing literature, the number of studies on forecasting oil price volatility was rather limited until the 2000's. Yet, the increase in crude oil price volatility observed around the period of the global financial crisis (see Figure 1)has created new interest into how to improve volatility forecasts. Reliable forecasts of oil price volatility are of interest for various economic agents, first and most obviously, for those firms whose business greatly depends on oil prices. Examples include oil companies that need to decide whether or not to drill a new well, airline companies who use oil price forecasts to set airfares, and the automobile industry. Second, they are useful for those whose daily task is to produce forecasts of industry-level and aggregate economic activity, such as central bankers, business economists, and private sector forecasters. Finally, oil price volatility also plays a role in households' decisions regarding purchases of durable goods, such as

---

[1]Chapter one is co-authored with Ana María Herrera of the University of Kentucky, and Liang Hu of Wayne State University

[2]See e.g. Alquist, Kilian and Vigfusson (2013) for a comprehensive study and a survey of the literature.

automobiles or heating systems (Kahn 1986, Davis and Kilian 2011, Plante and Traum 2012).

The aim of this paper is to provide a comprehensive and systematic examination of the conditional volatility (hereafter volatility) of daily crude oil spot prices. Traditionally, oil price volatility has been modeled as a time-invariant GARCH process.[3] Nonlinear GARCH models such as EGARCH (Nelson 1991) and GJR-GARCH (Glosten, Jagannathan and Runkle 1993) are well suited for this task as they are capable of capturing features such as volatility clustering, fat tails, and possible asymmetric effects. Furthermore, these models have been shown to have good out-of-sample performance when forecasting oil price volatility at short horizons (Mohammadi and Su 2010, and Hou and Suardi 2012). Nevertheless, oil prices are characterized by sudden jumps due to, for instance, political disruptions in the Middle East or military interventions in oil exporting countries. Markov switching models have been found to be better suited to model situations where changes in regimes are triggered by those sudden shocks to the economy. To the best of our knowledge, only two studies have addressed the possibility of changes in regime in oil price volatility: Fong and See (2002), and Nomikos and Pouliasis (2011). Both studies estimate Markov Switching GARCH (hereafter MS-GARCH) models to study the volatility of daily returns on oil futures, whereas the latter also estimates Mix-GARCH models.[4] Fong and See (2002) follow Gray's (1996) suggestion and integrate out the unobserved regime paths. Nomikos and Pouliasis (2011) use the estimation method proposed by Haas et al. (2004), where they simplify the regime shifting mechanism to make the estimation computationally tractable. The evidence found in favor of switching models is mixed. Fong and See's (2002) results suggest that GARCH-t[5] and MS-GARCH-t models are very close competitors when forecasting the one-step-ahead

---

[3]See Xu and Ouennich (2012) and references therein.

[4]The regime shifts are driven by i.i.d. mixture distributions, rather than by a Markov chain.

[5]t stands for Student's t distribution of the innovation.

volatility of daily GSCI oil futures. Instead, Nomikos and Pouliasis (2011) find that, for the one-step-ahead horizon, a Mix-GARCH-X[6] produces more accurate forecasts of the volatility in the returns of the NYMEX WTI oil futures.

In this paper, we model and forecast the volatility of the daily WTI closing spot price instead. One advantage of using this price to evaluate volatility forecasts is that it is available with no delay and it is not subject to revisions. This eliminates concerns regarding differences between real-time forecasts and forecasts produced with information that only becomes available after the forecast is generated. For instance, a researcher interested in forecasting the monthly volatility using the refiners acquisition cost (RAC) would have to deal with the issue that this price is released by the Energy Information Agency with a delay and that values for the previous months tend to be revised. In contrast, the forecast we produce using only the information contained in the history of the daily WTI closing spot price is the real-time forecast. Moreover, whereas financial investors might be more interested in volatility in crude oil futures, models that investigate the role of oil price volatility in economic activity and investment decisions focus more on spot oil prices.

This paper contributes to the literature in four important dimensions. First, we evaluate the role of regime switches in the volatility of daily returns on spot oil prices. To the best of our knowledge, such a research question has only been explored by Vo (2009), who uses weekly spot prices of WTI crude oil prices to estimate a Markov switching Stochastic Volatility (SV) model and finds that incorporating regime switching into a SV model enhances forecasting power. Given that spot oil prices exhibit sudden jumps and that MS-GARCH models are well suited to capture changes in regimes triggered by sudden shocks, evaluating their relative forecasting ability is of particular interest.

Second, in contrast with previous studies on crude oil price volatility, we formally test

---

[6]The GARCH-X model adds the squared lagged basis of futures prices to the GARCH specification of the conditional variance.

for regime switches using a testing procedure proposed by Carrasco, Hu, and Ploberger (2014). Testing for regime switching in GARCH models is especially important since it has been noted in the literature that the commonly found high persistence in the unconditional variance in financial series may be the result of neglected structural breaks or regime changes, see e.g., Lamoureux and Lastrapes (1990). In addition, Caporale, Pittis, and Spagnolo (2003) show via Monte Carlo studies that fitting (mis-specified) GARCH models to data generated by a MS-GARCH process tends to produce Integrated GARCH (IGARCH)[7] parameter estimates, leading to erroneous conclusions about the persistence levels. Indeed, we find overwhelming evidence in favor of a regime switching model for the daily crude oil price data.

Third, instead of following the estimation method of Gray (1996) or Haas et al. (2004), we use the technique developed by Klaassen (2002). This methodology makes efficient use of the conditional information when integrating out regimes to get rid of the path dependence. Furthermore, it has two advantages over Gray (1996): greater flexibility in capturing persistence of volatility shocks, and multi-step-ahead volatility forecasts that can be recursively calculated.[8] Meanwhile, a close look at Haas et al. (2004) reveals that their model has a simplified switching mechanism, where the regime switch occurs only in the GARCH effects. Our model, however, allows the conditional variance to switch to a different regime as well. For example, big shocks may be followed by a volatile period not only because of larger GARCH effects but also because of a possible switch to the higher variance regime. As a result, our model allows for more flexibility in modeling the volatility and persistence levels.

Last, but not least, we assess the out-of-sample forecasting performance of the different models using a battery of tests. We first follow Hansen and Lunde (2005) in considering

---

[7]The conditional variance grows with time t and the unconditional variance becomes infinity.

[8]By making multi-period ahead forecasts a convenient recursive procedure, Klaassen (2002) shows that MS-GARCH forecasts are better than single regime GARCH forecasts.

several statistical loss functions (e.g., mean square error, MSE, mean absolute deviation, MAD, quasi maximum likelihood, $QLike$) to evaluate out-of-sample forecasting performance, as no single criterion exists to select the best model when comparing volatility forecasts (Bollerslev et al. 1994, Lopez 2001). Then, we compute the Success Ratio (SR) and implement the Directional Accuracy (DA) tests from Pesaran and Timmermann (1992), conduct pairwise comparisons between different candidate models with Diebold and Mariano's (1995) test of Equal Predictive Ability, and groupwise comparisons using White's (2000) Reality Check test and Hansen's (2005) test of Superior Predictive Ability. Finally, we inquire into the stability of the forecasting accuracy for the preferred models over the evaluation period.

Our results suggest that EGARCH models yield more accurate out-of-sample forecasts at short horizons of 1 day and 5 days, whereas we generally favor MS-GARCH models at longer horizons. We also find overwhelming evidence that a normal innovation is insufficient to account for the leptokurtosis in our data, thus Student's t or GED distributions are more appropriate.[9] All in all, our results suggest that at longer horizons Markov switching models have superior predictive ability and yield more accurate forecasts than more restricted GARCH models where the parameters are time-invariant. Moreover, we uncover clear gains from using the MS-GARCH-t model for forecasting crude oil price volatility towards the end of the evaluation period at all horizons when comparing the mean squared prediction error ($MSPE$) of the preferred models.

ECONOMETRIC METHODOLOGY

This paper focuses on the out-of-sample forecasting performance of a variety of models for predicting oil price volatility. The models considered here belong to the conventional GARCH family or are Markov Switching GARCH models. This section describes these models.

---

[9]Our findings differ from Marcucci (2005) where normal innovation is favored in modeling financial returns.

Conventional GARCH Models

The ARCH model by Engle (1982) and the GARCH model by Bollerslev (1986) have been widely employed for modeling volatility in financial assets and oil prices. Thus, the first model we estimate is a standard GARCH$(1, 1)$ regression model:

$$
\begin{cases}
y_t = \mu_t + \varepsilon_t, \\
\varepsilon_t = \sqrt{h_t} \cdot \eta_t, \ \eta_t \sim iid(0, 1) \\
h_t = \alpha_0 + \alpha_1 \varepsilon_{t-1}^2 + \gamma_1 h_{t-1},
\end{cases}
\tag{1}
$$

where μ_t is the time-varying conditional mean possibly given by $\beta' \mathbf{x}_t$ with $\mathbf{x}_t$ being the $k \times 1$ vector of stochastic covariates. α_0, α_1 and γ_1 are all positive and $\alpha_1 + \gamma_1 \leq 1$.[10]

Denote the parameters of interest as $\theta = (\beta, \alpha_0, \alpha_1, \gamma_1)'$. Let $f(\eta_t; \nu)$ denote the density function for $\eta_t = \varepsilon_t(\theta)/\sqrt{h_t(\theta)}$ with mean 0, variance 1, and nuisance parameters $\nu \in \mathbb{R}^j$. The combined parameter vector is further denoted as $\psi = (\theta', \nu')'$. The likelihood function for the t-th observation is then given by

$$
f_t(y_t) = f_t(y_t; \psi) = \frac{1}{\sqrt{h_t(\theta)}} f\left(\frac{\varepsilon_t(\theta)}{\sqrt{h_t(\theta)}}; \nu \right).
\tag{2}
$$

The most commonly used distributions for η_t include the standard normal, the Student's t, and the Generalized Error Distribution (GED). Both Student's t and GED are able to capture extra leptokurtosis –which is commonly observed in financial returns and oil price returns–, yet they require one additional nuisance parameter ν to be estimated, e.g., the degrees of freedom in the Student's t and the shape parameter in the GED. Namely, if we assume η_t is standard normal, there are no additional nuisance parameters

---

[10]When $\alpha_1 + \gamma_1 = 1$, ε_t becomes an integrated GARCH (IGARCH) process, where a shock to the variance will remain in the system. However, it is still possible for it to come from a strictly stationary process, see Nelson (1990).

for the probability density function (pdf) and it is simply

$$f(\eta_t) = \frac{1}{\sqrt{2\pi}} \exp\left(-\frac{\eta_t^2}{2}\right). \tag{3}$$

Alternatively, if we assume η_t is distributed according to the Student's t distribution with ν degrees of freedom, the pdf of η_t is then given by

$$f(\eta_t; \nu) = \frac{\Gamma\left(\frac{\nu+1}{2}\right)}{\sqrt{(\nu-2)\pi}\Gamma\left(\frac{\nu}{2}\right)} \left(1 + \frac{\eta_t^2}{\nu-2}\right)^{-\frac{(\nu+1)}{2}}, \tag{4}$$

where $\Gamma(\cdot)$ is the Gamma function and ν is constrained to be greater than 2 so that the second moment exists and equals 1. If we assume a GED distribution, the pdf of η_t is modeled

$$f(\eta_t; \nu) = \frac{\nu \exp\left[-\frac{1}{2}\left|\frac{\eta_t}{\lambda}\right|^\nu\right]}{\lambda 2^{\left(1+\frac{1}{\nu}\right)}\Gamma\left(\frac{1}{\nu}\right)}, \tag{5}$$

with

$$\lambda \equiv \left[\frac{\left(2^{-\frac{2}{\nu}}\Gamma\left(\frac{1}{\nu}\right)\right)}{\Gamma\left(\frac{3}{\nu}\right)}\right]^{\frac{1}{2}},$$

where $\Gamma(\cdot)$ is again the Gamma function; ν is the shape parameter indicating the thickness of the tails and satisfying $0 < \nu < \infty$. When $\nu = 2$, the GED distribution becomes a standard normal distribution. If $\nu < 2$, the tails are thicker than normal. Once the distribution for η_t is specified, the parameter vector ψ can be estimated jointly using Maximum Likelihood Estimation (MLE).

A well-documented feature of financial data is the asymmetrical effects different types of shocks can have on volatility. For instance, political disruptions in the Middle East tend to increase volatility (see, e.g. Ferderer 1996, Wilson et al. 1996) whereas the effect of new oil field discoveries seems to have a more muted effect. Meanwhile, negative shocks seem to have a more pronounced effect on financial returns than positive shocks. The negative

correlation between current returns and future volatility is known as the leverage effect. In order to allow negative and positive shocks to have a different effect on the conditional variance of oil prices we estimate the GJR-GARCH developed by Glosten, Jagannathan, and Runkle (1993). The conditional variance is modeled as

$$h_t = \alpha_0 + \alpha_1 \varepsilon_{t-1}^2 + \xi \varepsilon_{t-1}^2 \mathcal{I}_{\{\varepsilon_{t-1} < 0\}} + \gamma_1 h_{t-1}, \tag{6}$$

where $\mathcal{I}_{\{\omega\}}$ is the indicator function equal to one if ω is true, and zero otherwise. Then the asymmetric effect is characterized by a positive ξ. ML estimation of GJR-GARCH can be conducted similarly under different distributional specifications.

Finally, a potential drawback of the standard GARCH model is the requirement that all of the parameters be positive. Nelson (1991) introduced the Exponential GARCH (EGARCH) model, which eliminated the non-negativity requirement. The logarithm of the conditional variance is described by

$$\log(h_t) = \alpha_0 + \alpha_1 \left(\left| \frac{\varepsilon_{t-1}}{\sqrt{h_{t-1}}} \right| - E \left| \frac{\varepsilon_{t-1}}{\sqrt{h_{t-1}}} \right| \right) + \xi \frac{\varepsilon_{t-1}}{\sqrt{h_{t-1}}} + \gamma_1 \log(h_{t-1}). \tag{7}$$

There are several interesting features of the EGARCH model. First, the equation for conditional variance is in log-linear form. Thus, the implied value of h_t can never be negative, permitting estimated coefficients to be negative. Second, the level of the standardized value of ε_{t-1}, $\left| \varepsilon_{t-1}/\sqrt{h_{t-1}} \right|$, is used instead of ε_{t-1}^2. As Nelson (1991) argues, this allows for a more natural interpretation of the size and persistence of shocks since the standardized value of ε_{t-1} is unit-less. Finally, the EGARCH model also allows for an asymmetric effect, which is measured by a negative ξ. The effect of a positive standardized shock on the logarithmic conditional variance is $\alpha_1 + \xi$; the effect of a negative standardized shock would be $\alpha_1 - \xi$ instead.

Notice that in the EGARCH, $E \left| \varepsilon_{t-1}/\sqrt{h_{t-1}} \right|$ takes different values under different

distribution specifications. When η_t is normal, $E\left|\varepsilon_{t-1}/\sqrt{h_{t-1}}\right|$ is the constant $\sqrt{\frac{2}{\pi}}$. Under the t distribution specified in (4),

$$E\left|\frac{\varepsilon_{t-1}}{\sqrt{h_{t-1}}}\right| = E\left|\eta_{t-1}\right| = \frac{2\sqrt{\nu-2}\Gamma\left(\frac{\nu+1}{2}\right)}{\sqrt{\pi}\cdot(\nu-1)\cdot\Gamma\left(\frac{\nu}{2}\right)}.$$

Under the GED distribution specified in (5),

$$E\left|\frac{\varepsilon_{t-1}}{\sqrt{h_{t-1}}}\right| = E\left|\eta_{t-1}\right| = \frac{\Gamma\left(\frac{2}{\nu}\right)}{\left[\Gamma\left(\frac{1}{\nu}\right)\Gamma\left(\frac{3}{\nu}\right)\right]^{1/2}}.$$

We simply plug these values in (7) and maximize the likelihood function across all parameters ψ in estimating EGARCH models.

MS-GARCH Models

As we mentioned in the introduction, a small number of studies have estimated MS-GARCH models to study the volatility of returns on oil price futures (see, e.g. Fong and See 2002, Nomikos and Pouliasis 2011). In fact, MS-GARCH models are of particular interest in the study of oil price volatility as the GARCH parameters are permitted to switch between regimes (e.g., periods that are perceived as of major political unrest versus periods of calm), thus providing flexibility over the standard GARCH models. For instance, a MS-GARCH model may better capture volatility persistence by allowing shocks to have a more persistent effect – through different GARCH parameters – during the high volatility regime and lower persistence during the low volatility regime. Meanwhile, MS-GARCH models can also capture the pressure-relieving effects of some large shocks, which may occur when large shocks that are not persistent are followed by relatively tranquil periods rather than by a switch to a higher volatility regime. Thus, a regime-switching model is flexible enough to accommodate volatility clustering and different levels of volatility persistence (Klaassen 2002).

We consider the MS-GARCH$(1, 1)$ model given by

$$
\begin{cases}
y_t = \mu^{S_t} + \varepsilon_t, \\
\varepsilon_t = \sqrt{h_t} \cdot \eta_t, \ \eta_t \sim iid(0, 1) \\
h_t = \alpha_0^{S_t} + \alpha_1^{S_t} \varepsilon_{t-1}^2 + \gamma_1^{S_t} h_{t-1},
\end{cases}
\tag{8}
$$

where we allow both the conditional mean μ^{S_t} and the conditional variance h_t to be subject to a hidden Markov chain, S_t. In this paper, we focus on a two-state first-order Markov chain. That is, the transition probability of the current state only depends on the most adjacent past state:

$$
P\left(S_t \mid S_{t-1}, \mathcal{I}_{t-2}\right) = P\left(S_t \mid S_{t-1}\right),
$$

where $\mathcal{I}_{t-2}$ denotes the information set up to $t - 2$. We use p_{ij} to denote the transition probability that state i is followed by state j. We assume the Markov chain is geometric ergodic. More precisely, if S_t takes two values 1 and 2, and has transition probabilities $p_{11} = P\left(S_t = 1 \mid S_{t-1} = 1\right)$ and $p_{22} = P\left(S_t = 2 \mid S_{t-1} = 2\right)$, S_t is geometric ergodic if $0 < p_{11} < 1$ and $0 < p_{22} < 1$.

Estimating the model in (8) is computationally intractable, because the conditional variance h_t depends on the state-dependent h_{t-1}, consequently on all past states. Maximizing the likelihood function would require integrating out all possible unobserved regime paths, which grow exponentially with sample size T. Gray (1996) suggests integrating out the unobserved regime path $\tilde{S}_{t-1} = (S_{t-1}, S_{t-2}, ...)$ to avoid the path dependence, namely, replacing the path-dependent h_{t-1} by

$$
\begin{aligned}
h_{t-1} \ = \ & E_{t-2}\left[h_{t-1}^{(i)}\right] = p_{1,t-1}\left[\left(\mu_{t-1}^{(1)}\right)^2 + h_{t-1}^{(1)}\right] + p_{2,t-1}\left[\left(\mu_{t-1}^{(2)}\right)^2 + h_{t-1}^{(2)}\right] \\
& - \left[p_{1,t-1}\mu_{t-1}^{(1)} + p_{2,t-1}\mu_{t-1}^{(2)}\right]^2,
\end{aligned}
$$

where $h_{t-1}^{(i)}$ and $\mu_{t-1}^{(i)}$ represent the the conditional variance and mean at time $t-1$ in state i, respectively, and $p_{1,t-1} = P(S_{t-1} = 1 \mid \mathcal{I}_{t-2})$ and $p_{2,t-1} = P(S_{t-1} = 2 \mid \mathcal{I}_{t-2})$ are the *ex-ante* probabilities. This specification avoids the path dependence issue and makes estimation very straightforward. But the disadvantage is that multi-step-ahead forecasting is very complicated.

In this paper we follow Klaassen (2002) and Marcucci (2005) and replace h_{t-1} by its expectation conditional on the information set at $t-1$ plus the current state variable, namely,

$$h_t^{(i)} = \alpha_0^{(i)} + \alpha_1^{(i)}\varepsilon_{t-1}^2 + \gamma_1^{(i)} E_{t-1}\left[h_{t-1}^{(i)} \mid S_t\right],$$

where

$$E_{t-1}\left[h_{t-1}^{(i)} \mid S_t\right] = \sum_{j=1}^{2} p_{ji,t-1}\left[\left(\mu_{t-1}^{(j)}\right)^2 + h_{t-1}^{(j)}\right] - \left[\sum_{j=1}^{2} p_{ji,t-1}\mu_{t-1}^{(j)}\right]^2,$$

and $p_{ji,t-1} = P\left(S_{t-1} = j \mid S_t = i, \mathcal{I}_{t-2}\right)$, $i, j = 1, 2$, and calculated as

$$p_{ji,t-1} = \frac{p_{ji}\Pr(S_{t-1} = j \mid \mathcal{I}_{t-2})}{\Pr(S_t = i \mid \mathcal{I}_{t-2})} = \frac{p_{ji}p_{j,t-1}}{\sum_{j=1}^{2} p_{ji}p_{j,t-1}}.$$

Similar to Gray (1996), this specification circumvents the path dependence by integrating out the path-dependent h_{t-1}. However, it uses the information set at time $t-1$ plus the current state S_t, which embodies Gray's $\mathcal{I}_{t-2}$ information set. Given that regimes are often observed to be highly persistent, S_t contains lots of information about S_{t-1}. Klaassen (2002) discovers that an empirical advantage of this specification over Gray's is the efficient use of all information available to the researcher. It also has the theoretical advantage of entailing a straightforward computation of the m-step-ahead volatility

forecasts at time T as follows[11]:

$$\hat{h}_{T,T+m} = \sum_{\tau=1}^{m} \hat{h}_{T,T+\tau} = \sum_{\tau=1}^{m} \sum_{i=1}^{2} P(S_{T+\tau} = i \mid \mathcal{I}_T) \hat{h}_{T,T+\tau}^{(i)},$$

where the τ-step-ahead volatility forecast in regime i made at time T can be calculated recursively

$$\hat{h}_{T,T+\tau}^{(i)} = \alpha_0^{(i)} + \left(\alpha_1^{(i)} + \gamma_1^{(i)} \right) E_T \left[h_{T,T+\tau-1}^{(i)} \mid S_{T+\tau} \right].$$

Parameter estimates can be obtained by maximizing the log likelihood function

$$\mathcal{L} = \sum_{t=1}^{T} \log \left[p_{1,t} f_t(y_t \mid S_t = 1) + p_{2,t} f_t(y_t \mid S_t = 2) \right],$$

where $f_t(y_t \mid S_t = i)$ is the conditional density of y_t given regime i occurs at time t, and the ex-ante probabilities $p_{j,t}$ are calculated as

$$p_{j,t} = \Pr(S_t = j \mid \mathcal{I}_{t-1}) = \sum_{i=1}^{2} p_{ij} \frac{f_{t-1}(y_{t-1} \mid S_{t-1} = i) p_{i,t-1}}{\sum_{k=1}^{2} f_{t-1}(y_{t-1} \mid S_{t-1} = k) p_{k,t-1}}, j = 1, 2.$$

The estimation method used here differs from other studies of oil price volatility that estimate MS-GARCH models. In particular, Fong and See (2002) follow Gray's (1996) suggestion and integrate out the unobserved regime paths. Nomikos and Pouliasis (2011) use the estimation method proposed by Haas et al. (2004) instead, where they simplify the regime shift mechanism to make the estimation computationally tractable. Our estimation method can be applied to the general MS-GARCH model, meanwhile making efficient use of the conditional information when integrating out regimes.

Since oil price returns exhibit similar characteristics to common financial returns, and to maintain comparability between the GARCH and MS-GARCH models, we also consider

---

[11]m-step-ahead volatility is the summation of the volatility at each step because of absence of serial correlation in returns.

three different types of distributions for η_t: normal, Student's t, and GED distributions.

DATA DESCRIPTION

We use the daily spot price for the West Texas Intermediate (WTI) crude oil obtained from the U.S. Energy Information Administration. The sample period ranges from January 2, 1986 to April 5, 2013. Thus we have 6877 observations. Over this period of time, the average price for a barrel of crude oil was $39.26, the median value equaled $24.48, and the standard deviation was $28.82. A maximum price of $145.31 was observed on July 3, 2008; this record high was possibly a consequence of geopolitical tensions over Iranian missile tests. To model the returns in the oil price and its volatility, we calculate daily oil returns by taking 100 times the difference in the logarithm of consecutive days' closing prices. Table 1 shows the descriptive statistics for WTI rates of return. The mean rate of return is about 0.0187 with a standard deviation of 2.56. Note also that WTI returns are negatively skewed. Kurtosis is extremely high at the value of 17.70, compared with 3 for a normal distribution. These findings are consistent with previous studies by, e.g., Abosedra and Laopodis (1997), Morana (2001), Bina and Vo (2007), among others. Figure 1 plots the returns of the WTI spot prices and the squared deviations over the sample period. Large variations are observed during the period of the crude oil price collapse in 1986, the Iraq-Kuwait war in late 1990 and early 1991, the crude oil price crisis of 1998, as well as in the midst of the financial crisis in late 2008. Indeed, Figure 1 suggests crude oil returns are characterized by periods of low volatility followed by high volatility in the face of major political or financial unrest.

In this paper we are interested in forecasting volatility. Two questions are of relevance here: (i) How do we measure volatility? (ii) How do we evaluate the relative forecasting performance of alternative models? We focus on the first question in this section and deal with the second question in Section 5. The main issue is that the true volatility σ_t^2 is not observable. Therefore, we need to compute some proxy for the true volatility.
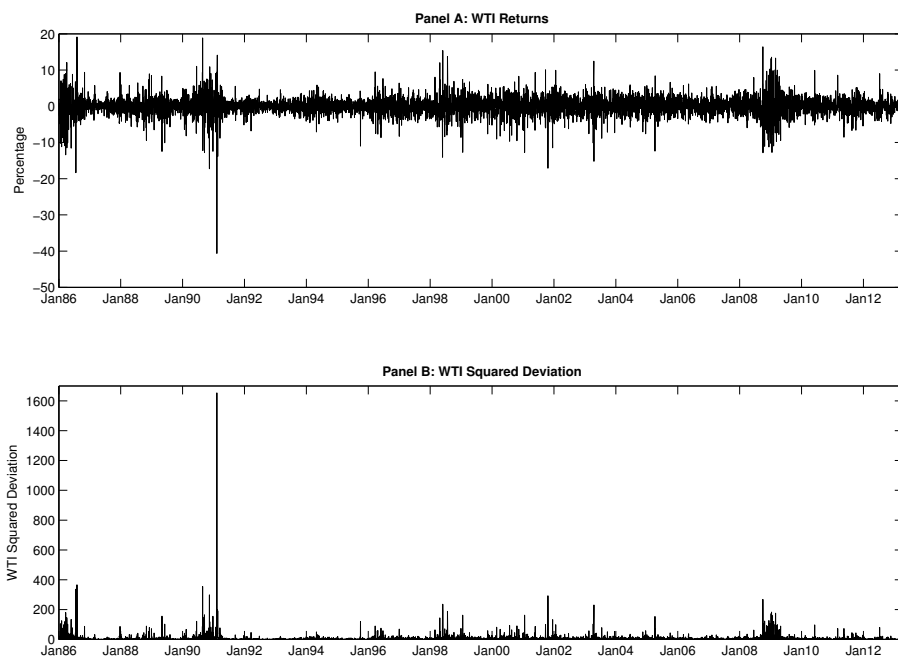
Figure 1: Daily WTI Crude Oil Returns and Squared Deviations. The sample period extends from January 2, 1986 through April 5, 2013.

Descriptive Statistics

			WTI Returns			
Mean	Std. Dev	Min	Max	Variance	Skewness	Kurtosis
0.0187	2.56	-40.64	19.15	6.57	-0.76	17.70

			$RV^{1/2}$			
Mean	Std. Dev	Min	Max	Variance	Skewness	Kurtosis
0.021	0.014	0.0035	0.41	0.00021	6.70	112.35

			$\ln(RV^{1/2})$			
Mean	Std. Dev	Min	Max	Variance	Skewness	Kurtosis
-3.98	0.48	-5.65	-0.90	0.23	0.58	4.50

Table 1: Note: WTI returns are over the sample period of January 2, 1986 to April 5, 2013 for 6876 observations. $RV^{1/2}$, and the natural logarithm of $RV^{1/2}$ series are from January 5,1987 to April 5, 2013 for 6580 observations.

It seems natural to use the squared daily returns as a proxy. However, it has been noted in the literature (e.g. Andersen and Bollerslev 1998) that this is a noisy estimate of the true volatility. To see this, we can rewrite model (1) as $\varepsilon_t^2 = h_t \cdot \eta_t^2 = h_t + (\eta_t^2 - 1)h_t$. Leptokurtosis in the data suggests that the idiosyncratic component η_t would contribute a large amount of noise relative to the underlying volatility. In fact, this noise can lead to improper conclusions about the ability of the GARCH models to forecast volatility. Fortunately, the availability of high frequency futures data helps to solve this issue. We follow Andersen and Bollerslev (1998) and compute realized volatility using the sum of intraday squared futures returns at 5 minutes as our proxy of true volatility instead. Anderson et al. (2003) establish the theoretical justification for the realized volatility as an accurate measure of the underlying volatility. Furthermore, Andersen and Bollerslev (1998) test a variety of sampling frequencies for foreign exchange data to show that the realized volatility measure converges to the true volatility as the frequency of observation increases. However, they also find increasing the sampling frequency to less than 5 minutes has practical limitations due to market microstructure noise and discrete price observations. They determine 5-minute intraday returns are the best frequency for calculating their realized volatility measure. Liu, Patton, and Sheppard (2012) among others, also find that the 5-minute sampling frequency outperforms most other realized volatility measures across multiple asset classes including equities and interest rates.

Therefore, to compute our measure of realized volatility for the out-of-sample evaluation we obtained the oil futures[12] series from TickData.com. We downloaded 5-minute prices of 1-month futures contracts during the NYSE trading hours (9:30am to 4:00pm EST, Monday through Friday), excluding market holidays from January 5, 1987 (when this futures contract started trading) to April 5, 2013. Following Blair, Poon, and Taylor (2001), we constructed the daily realized volatility RV_t by summing the squared 5-minute

---

[12]NYMEX Light Sweet Crude Oil, symbol CL.

returns during trading hours and then adding the square of the previous "overnight" return.[13]

We list the summary statistics for both the $RV_t^{1/2}$ and the logarithm of $RV_t^{1/2}$ in Table 1. The $RV_t^{1/2}$ series is severely right-skewed and leptokurtic. However, the logarithmic series appears much closer to a normal distribution, which is further confirmed by comparing its kernel density estimates with the normal distribution in Figure 2.[14]
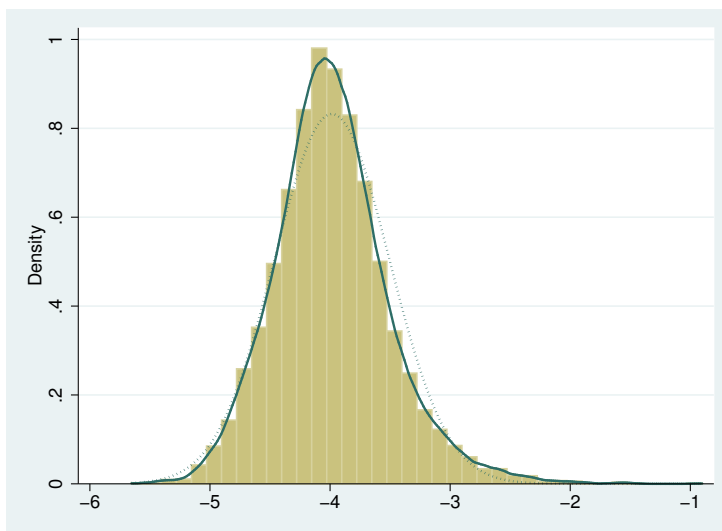
Figure 2: $\ln(RV^{1/2})$ distributions. The sample period extends from January 5, 1987 through April 5, 2013. The solid line is the kernel density. The dotted line is a normal density scaled to have the same mean and standard deviation of the data.

We then evaluate the forecasting performance of various GARCH and MS-GARCH models with the realized volatility as reference. Since the forecasts will be utilized by

[13]Hansen and Lunde (2005) suggest an alternative way to measure the daily realized volatility. They first calculate the constant $\widehat{c} = [n^{-1} \sum_{t=1}^{n} (r_t - \widehat{\mu})^2]/[n^{-1} \sum_{t=1}^{n} rv_t]$, where r_t and $\widehat{\mu}$ are the close-to-close return of the daily prices and the mean respectively, and rv_t is the 5-minute realized volatility during the trading hours only. Then they scale the realized volatility rv_t by the constant $\widehat{c}$. This measure is less noisy compared with directly adding the overnight returns. However, it is not suitable here since the value for $\widehat{c}$ varies with sub-samples for our data series. For instance, prior to 7/1/2003, oil futures were traded from 10:00am until 2:30pm and $\widehat{c} = 1.19$. After 7/1/2003, trading hours were expanded to the entire day, with the exception of a 45-minute period from 5:15pm to 6:00pm when trading is halted. For the sub-sample of 7/1/2003 to 4/5/2013, $\widehat{c} = 1.85$. If instead we focus on the sample period 1/2/1992 to 1/31/1997 from Fong and See (2002), $\widehat{c} = 1.03$, whereas if we use the sample period 1/23/1991 to 12/31/1997 from Nomikos and Pouliasis (2011), $\widehat{c} = 1.33$. Finally, for our out-of-sample period 1/3/2012 to 4/5/2013, $\widehat{c} = 2.33$.

[14]Anderson et al. (2003) have similar findings for the realized volatility on exchange rates.

agents who have differing investment horizons, we evaluate relative forecasting performance of the different models at various horizons. For example, central bankers typically need a monthly forecast. Oil exploration and production firms might be interested in longer horizons and this horizon might vary across regions. For instance, while the time to complete oil wells averages 20 days in Texas, it averages 90 days in Alaska. Therefore, we focus on 4 forecasting horizons at $m = 1$, 5, 22, and 66 days, corresponding to 1 day, 1 week, 1 month and 3 months respectively. Then, to calculate m-step-ahead realized volatility at time T, we simply sum the daily realized volatility over m days, denoted by:

$$\widehat{RV}_{T,T+m} = \sum_{j=1}^{m} \widehat{RV}_{T+j}.$$

We divide the whole sample into two parts: the first 6560 observations (corresponding to a period of January 2, 1986 to December 30, 2011) are used for in-sample estimation, while the remaining observations are used for out-of-sample forecast evaluation in the year 2012.[15]

ESTIMATION RESULTS

We regress the daily returns on a constant, and test the residuals for autocorrelations and ARCH effects. The Breusch-Godfrey test cannot reject the null of no serial autocorrelation.[16] However, the LM test for ARCH effects strongly rejects the null of no ARCH effect in all lag orders from 1 to 20.[17] So we start estimating our model with the conditional mean $r_t = \mu + \varepsilon_t$.

GARCH

The ML estimates for GARCH$(1,1)$, EGARCH$(1,1)$, and GJR-GARCH$(1,1)$ models are collected in Table 2. For each model, we report the results with Normal, Student's t,

---

[15] Our observations extend to April 5, 2013 to accommdate the m-step-ahead forecast at $m = 66$.
[16] p-value is 0.413.
[17] $p-$values are all at 0.

<div align="center">MLE Estimates of Standard GARCH Models</div>

	GARCH			EGARCH			GJR		
	N	t	GED	N	t	GED	N	t	GED
μ	0.0325	0.0634**	0.0596**	0.0323	0.0542**	0.0535**	0.0366	0.0582**	0.0575**
	(0.0217)	(0.0230)	(0.0219)	(0.0227)	(0.0227)	(0.0219)	(0.0239)	(0.0230)	(0.0222)
α_0	0.0895**	0.0754**	0.0799**	0.0311**	0.0177**	0.0187**	0.0723**	0.0684**	0.0679**
	(0.0095)	(0.0120)	(0.0134)	(0.0031)	(0.0041)	(0.0043)	(0.0093)	(0.0134)	(0.0133)
α_1	0.0938**	0.0645**	0.0739**	0.1976**	0.1413**	0.1610**	0.0990**	0.0584**	0.0719**
	(0.0039)	(0.0060)	(0.0063)	(0.0072)	(0.0117)	(0.0118)	(0.0045)	(0.0083)	(0.0078)
γ_1	0.8952**	0.9225**	0.9130**	0.9869**	0.9886**	0.9880**	0.8996**	0.9230**	0.9165**
	(0.0046)	(0.0070)	(0.0070)	(0.0017)	(0.0024)	(0.0025)	(0.0046)	(0.0068)	(0.0067)
ξ	-	-	-	-0.0036	-0.0129*	-0.0138*	-0.0082	0.0164	0.0040
				(0.0040)	(0.0075)	(0.0069)	(0.0061)	(0.0107)	(0.0099)
ν	-	6.0212**	1.3238**	-	5.9813**	1.3213**	-	5.9370**	1.3224**
		(0.3930)	(0.0229)		(0.3845)	(0.0229)		(0.3896)	(0.0239)
$Log(L)$	-14617.958	-14394.203	-14430.459	-14607.225	-14373.253	-14415.257	-14615.477	-14391.249	-14427.854

Table 2: Note: * and ** represent significance at 5% and 1% level respectively. A one-sided test is conducted on ξ. Each model is estimated with Normal, Student's t, and GED distributions. The in-sample data consist of WTI returns from 1/2/1986 to 12/31/11. The conditional mean is $r_t = \mu + \varepsilon_t$. The conditional variances are $h_t = \alpha_0 + \alpha_1 \varepsilon_{t-1}^2 + \gamma_1 h_{t-1}$, $\log(h_t) = \alpha_0 + \alpha_1 \left(\left| \frac{\varepsilon_{t-1}}{\sqrt{h_{t-1}}} \right| - E \left| \frac{\varepsilon_{t-1}}{\sqrt{h_{t-1}}} \right| \right) + \xi \frac{\varepsilon_{t-1}}{\sqrt{h_{t-1}}} + \gamma_1 \log(h_{t-1})$, and $h_t = \alpha_0 + \alpha_1 \varepsilon_{t-1}^2 + \xi \varepsilon_{t-1}^2 I_{\{\varepsilon_{t-1<0}\}} + \gamma_1 h_{t-1}$ for GARCH, EGARCH, and GJR-GARCH respectively. Asymptotic standard errors are in parenthesis.

and GED innovations. Asymptotic standard errors are reported in parentheses.[18]

In using a normal innovation, the conditional mean in all three models is insignificant at the 5% level. When a t or GED distribution is used, the conditional mean is significantly positive at around 0.06. Recall that the kurtosis of this return series is 17.86 from Table 1. Moreover, the degrees of freedom for the t distribution are estimated at around 6 in all three GARCH models[19] and the estimated shape parameter for GED distribution is

---

[18]The Maximum Likelihood estimates are obtained using the MATLAB's numerical optimization routine FMINCON. We use the nonlinear Sequential Quadratic Programming (SQP) method with FMINCON to jointly estimate the conditional mean and conditional variance by maximizing the log-likelihood function. SQP closely mimics Newton's method for constrained optimization. For each iteration the Hessian of the Lagrangian function is updated using the BFGS quasi-Newton method.

[19]This suggests that the conditional moments exist up to the 6th order. Morever, since the conditional kurtosis for the t distribution is calculated by $3(\nu - 2)/(\nu - 4)$, $\nu = 6$ implies much fatter tails than normal distributions.

around 1.32[20], which is consistent with the common finding in the literature that the normal error might not be able to account for all the mass in the tails in the distributions of daily returns.

In EGARCH-t and EGARCH-GED, the asymmetric effect (ξ) is significantly negative at 5%, suggesting that a negative shock would increase the future conditional variance more than a positive shock of the same magnitude. However, this asymmetric effect is not significant across all GJR specifications.

The estimates of the variance parameters reveal high persistence levels (indicated by $\alpha_1 + \gamma_1$ close to 1) throughout the GARCH specifications. In GJR and EGARCH models, the persistence levels are measured by $\alpha_1 + \gamma_1 + 0.5\xi$ and γ_1 instead. The estimates are also very close to 1, suggesting high persistence in all cases.

MS-GARCH

Studies that estimate MS-GARCH models for oil price returns (e.g. Fong and See 2002, Vo 2009, and Nomikos and Pouliasis 2011) or a stock price index (e.g. Marcucci 2005), proceed to estimate the MS-GARCH models without testing for the existence of regime switching. In fact, testing for Markov switching in GARCH models is complicated mainly for two reasons. First, the GARCH model itself is highly nonlinear. When the parameters are subject to regime switching, path dependence together with nonlinearity makes the estimation intractable, consequently (log) likelihood functions are not calculable. Second, standard tests suffer from the famous Davies problem, where the nuisance parameters characterizing the regime switching are not identified under the null. Therefore, standard tests like the Wald or LR test do not have the usual Chi-squared distribution. Markov switching tests by e.g., Hansen (1992) or Garcia (1998) are not applicable here either since they both involve examining the distribution of the likelihood ratio statistic, which is not feasible for MS-GARCH. We adopt the testing procedure developed by Carrasco,

---

[20]The kurtosis for the GED distribution is given by $\left(\Gamma\left(1/\nu\right)\Gamma\left(5/\nu\right)\right)/\Gamma^2\left(3/\nu\right)$. When $\nu = 1.32$, the kurtosis is at 4.27, again confirming fat tails.

Hu, and Ploberger (2014, CHP test thereafter). The advantage of this test is that it only requires estimating the model under the null hypothesis of constant parameters, yet the test is still optimal in the sense that it is asymptotically equivalent to the LR test. In addition, it has the flexibility to test for regime switching in both the means and the variances or any subset of these parameters. We describe in detail how to conduct their test for regime switching in mean and variances. Specifically, the model under the null hypothesis (H_0) is (1) where $\mu_t = \mu$ and the alternative (H_1) model is (8).

Given our model, the (conditional) log likelihood function under H_0 is

$$l_t = -\frac{1}{2}\ln 2\pi - \frac{1}{2}\ln\left(\alpha_0 + \alpha_1\varepsilon_{t-1}^2 + \gamma_1 h_{t-1}\right) - \frac{(y_t - \mu)^2}{2\left(\alpha_0 + \alpha_1\varepsilon_{t-1}^2 + \gamma_1 h_{t-1}\right)}. \tag{9}$$

We first obtain the MLE for the parameters $\hat{\theta}$ under H_0, where $\theta = (\mu, \alpha_0, \alpha_1, \gamma_1)'$. Then, we calculate the first and second derivatives of the log likelihood (9) with respect to θ evaluated at $\hat{\theta}$. The nuisance parameters specifying the Markov switching are not identified under H_0. Nevertheless, we denote the parameters as $\zeta = (h, \rho : \|h\| = 1, -1 < \underline{\rho} < \rho < \bar{\rho} < 1)$, where h is normalized and characterizes the direction of the alternative and ρ specifies the autocorrelation of the Markov chain. Given ζ, the first key component of the CHP test is $\Gamma_T^* = \sum \mu_{2,t}\left(\zeta, \hat{\theta}\right)/\sqrt{T}$, where

$$\mu_{2,t}\left(\zeta, \hat{\theta}\right) = \frac{1}{2}h'\left[\left(\frac{\partial^2 l_t}{\partial\theta\partial\theta'} + \left(\frac{\partial l_t}{\partial\theta}\right)\left(\frac{\partial l_t}{\partial\theta}\right)'\right) + 2\sum_{s<t}\rho^{(t-s)}\left(\frac{\partial l_t}{\partial\theta}\right)\left(\frac{\partial l_s}{\partial\theta}\right)'\right]h.$$

The second component is $\widehat{\epsilon}^*$, which is the residual of the regression of $\mu_{2,t}\left(\zeta, \hat{\theta}\right)$ on $l_t^{(1)}\left(\hat{\theta}\right)$. Then the sup test simply takes the form:

$$\text{supTS} = \sup_{\{h,\rho:\|h\|=1,\underline{\rho}<\rho<\bar{\rho}\}} \frac{1}{2}\left(\max\left(0, \frac{\Gamma_T^*}{\sqrt{\widehat{\epsilon}^{*\prime}\widehat{\epsilon}^*}}\right)\right)^2. \tag{10}$$

Alternatively, the exp test is:

$$\text{expTS} = \underset{\{h,\rho:\|h\|=1,\underline{\rho}<\rho<\bar{\rho}\}}{avg} \Psi\left(h,\rho\right),$$

where

$$\Psi\left(h,\rho\right) = \begin{cases} \sqrt{2\pi}\exp\left[\frac{1}{2}\left(\frac{\Gamma_T^*}{\sqrt{\widehat{\epsilon}^{*\prime}\widehat{\epsilon}^*}}-1\right)^2\right]\Phi\left(\frac{\Gamma_T^*}{\sqrt{\widehat{\epsilon}^{*\prime}\widehat{\epsilon}^*}}-1\right) & \text{if } \widehat{\epsilon}^{*\prime}\widehat{\epsilon}^* \neq 0, \\ 1 & \text{otherwise.} \end{cases}$$

That is, the unidentified nuisance parameters ζ are integrated out with respect to some priors in the supremum or exponential form to deliver an optimal test in the Bayesian sense.

We generate the 4×1 vector h uniformly over the unit sphere 60 times, corresponding to the switching mean and the three GARCH parameters.[21] The supTS is maximized over h and a grid search of ρ on the interval $[-0.95, 0.95]$ with the step length of 0.05. Meanwhile, expTS is the average of $\Psi\left(h,\rho\right)$ above computed over those h and $\rho's$. For our data, the sup and exp test statistics are calculated to be 0.00522 and 0.675, respectively. Then we simulate the critical values by bootstrapping using 1,000 iterations. We reject the null of constant parameters in favor of regime switching in both the mean and variance equations with p-values of 0 for both supTS and expTS. These results show overwhelming support for a Markov switching model. Hence we estimate the MS-GARCH models with a two-state Markov chain. Table 3 presents the parameter estimates for the three MS-GARCH models: MS-GARCH-N, MS-GARCH-t, and MS-GARCH-GED, respectively.

Again with normal innovations, the results are not robust. For example, $\alpha_1^{(2)}$ is insignificantly different from 0, casting doubt upon the validity of the GARCH specification in this regime. Thus we focus on MS-GARCH-t and MS-GARCH-GED instead. The results are quite similar. In both models, regime 1 corresponds to a significantly positive

---

[21]To test for switching in the variance equation only, we can simply set the first element of h to be 0 and generate the remaining 3×1 vector uniformly over the unit sphere.

Maximum Likelihood Estimates of MS-GARCH Models

	MS-GARCH-N	MS-GARCH-t	MS-GARCH-GED
$\mu^{(1)}$	0.0729**	0.1148**	0.1150**
	(0.0247)	(0.0353)	(0.0330)
$\mu^{(2)}$	-0.3103**	0.0158	0.0093
	(0.1200)	(0.0337)	(0.0323)
$\sigma^{(1)}$	1.1239**	2.3263**	2.3630**
	(0.0351)	(0.0234)	(0.0254)
$\sigma^{(2)}$	42.7112**	2.5890**	2.9275**
	(0.3814)	(0.0212)	(0.0225)
$\alpha_1^{(1)}$	0.0420**	0.0214**	0.0265**
	(0.0149)	(0.0069)	(0.0072)
$\alpha_1^{(2)}$	4.27 E-09	0.1366**	0.1562**
	(0.0116)	(0.0212)	(0.0207)
$\gamma_1^{(1)}$	0.8053**	0.9616**	0.9550**
	(0.0131)	(0.0089)	(0.0091)
$\gamma_1^{(2)}$	0.9983**	0.8486**	0.8324**
	(0.0131)	(0.0206)	(0.0203)
p_{11}	0.9459**	0.9970**	0.9974**
	(0.0058)	(0.0016)	(0.0013)
p_{22}	0.7158**	0.9951**	0.9959**
	(0.0338)	(0.0024)	(0.0019)
ν	-	6.2133**	1.3506**
		(0.4160)	(0.0256)
$Log(L)$	-14520.17	-14373.95	-14410.13
$N.of\ Par.$	10	11	11
π_1	0.8401	0.6203	0.6119
π_2	0.1599	0.3797	0.3881
$\alpha_1^{(1)} + \gamma_1^{(1)}$	0.8473	0.9830	0.9815
$\alpha_1^{(2)} + \gamma_1^{(2)}$	0.9983	0.9852	0.9886

Table 3: Note: * and ** represent significance at 5% and 1% level respectively. Each MS-GARCH model is estimated using different distribution as described in the text. The in-sample data consist of WTI returns from 1/2/1986 to 12/31/11. The superscripts indicate the regime. The standard deviation conditional on the regime is reported: $\sigma^{(i)} = \left(\alpha_0^{(i)} / (1 - \alpha_1^{(i)} - \gamma_1^{(i)}) \right)^{1/2}$. π_i is the ergodic probability of being in regime i; $\alpha_1^{(i)} + \gamma_1^{(i)}$ measures the persistence of shocks in the i-th regime. Asymptotic standard errors are in the parentheses.

mean, while the conditional mean in regime 2 is insignificantly different from 0. The transition probabilities, p_{11} and p_{22}, are significant and close to one, implying that both regimes are highly persistent. However, the ergodic probabilities suggest that regime 1 occurs more often. About 62% of the observations are in regime 1, with the remaining 38% in regime 2. Moreover, regime 1 has a lower standard deviation than regime 2. In summary, we could call regime 1 –where most of the observations are located– the "good regime", with positive expected returns and lower volatility. In contrast, regime 2 is a "bad regime", where zero expected return is accompanied by higher volatility.

FORECAST EVALUATION

A Description of the Forecast Evaluation Methods

We compute 251 out-of-sample volatility forecasts (corresponding to the year 2012) for the 1-, 5-, 22-, and 66-step horizons using a rolling sample period. That is, we use the first 6560 daily observations spanning the period between January 2, 1986 and December 30, 2011 to estimate the volatility models; these estimates are then used to compute the forecasts at all horizons for the first out-of-sample period, January 3, 2012. We move to the next window by adding an observation at the end of the estimation period and drop an observation at the beginning, re-estimate our parameters, and compute a new forecast. We first present a description of the tests we employ and then an evaluation of the forecasts.

Statistical Loss Functions

Given that there is no unique criterion to select the best model when comparing volatility forecasts (see Bollerslev et al. 1994 and Lopez 2001), we follow Hansen and Lunde (2005) in computing six different loss functions for forecast evaluation. The use of various statistical functions has the advantage of allowing for a more systematic and complete comparison of the alternative forecast models. Given the volatility σ_t^2 and its model forecast $\hat{h}_t$, the first two criteria are the usual mean squared error (MSE) functions

given by

$$MSE_1 = n^{-1} \sum_{t=1}^{n} \left(\sigma_t - \hat{h}_t^{1/2} \right)^2 \tag{11}$$

and

$$MSE_2 = n^{-1} \sum_{t=1}^{n} \left(\sigma_t^2 - \hat{h}_t \right)^2. \tag{12}$$

We also compute two Mean Absolute Deviation (MAD) functions, as these criteria are more robust to outliers than the MSE functions. These are given by

$$MAD_1 = n^{-1} \sum_{t=1}^{n} \left| \sigma_t - \hat{h}_t^{1/2} \right|, \tag{13}$$

$$MAD_2 = n^{-1} \sum_{t=1}^{n} \left| \sigma_t^2 - \hat{h}_t \right|. \tag{14}$$

Two disadvantages of the MAD are that they treat positive and negative errors symmetrically and they are not invariant to scale transformations.

The last two criteria are the $R^2 LOG$ and the $QLIKE$:

$$R^2 LOG = n^{-1} \sum_{t=1}^{n} \left[\log(\sigma_t^2 \hat{h}_t^{-1}) \right]^2, \tag{15}$$

$$QLIKE = n^{-1} \sum_{t=1}^{n} \left(\log \hat{h}_t + \sigma_t^2 \hat{h}_t^{-1} \right). \tag{16}$$

Equation (15) represents the logarithmic loss function of Pagan and Schwert (1990). It is similar to the R^2 from a regression of the squared first difference of the logged oil price on the conditional variance, and it penalizes volatility forecasts asymmetrically in low and high volatility regimes. The $QLIKE$ is equivalent to the loss implied by a Gaussian likelihood.

Success Ratio and Directional Accuracy

We employ several methods to evaluate the relative forecasting performance of the different models. First, to evaluate the ability of the models to predict the direction of the change in the volatility, we calculate the Success Ratio (SR), which is the percentage of times the volatility forecasts move in the same direction as the actual volatility. Evaluating the proportion of times the direction of change in the volatility forecasts are correctly predicted is key for consumers of oil forecasts[22] because increases and decreases in volatility might have asymmetric effects on economic activity. Furthermore, we apply the Directional Accuracy (DA) test of Pesaran and Timmermann (1992), which is constructed as a standardized statistic for SR and is asymptotically distributed as standard normal.

Using RV_t as a proxy for σ_t^2, the percentage of times the volatility forecasts move in the same direction as realized volatility is given by:

$$SR = n^{-1} \sum_{t=1}^{n} \mathcal{I}_{\left\{\overline{RV}_t \cdot \bar{h}_t > 0\right\}}, \tag{17}$$

where $\overline{RV}_t$ is the demeaned realized volatility proxy at t, and $\bar{h}_t$ is the demeaned volatility forecast at t. If the realized volatility and the forecasted volatility move in the same direction, then $\mathcal{I}_{\{\omega>0\}}$ is equal to 1; 0 otherwise.

Having computed the SR, we calculate $SRI = P\widehat{P} + (1 - P)(1 - \widehat{P})$ where P is the fraction of times that $\overline{RV}_t$ is positive and $\widehat{P}$ is the fraction of times that $\bar{h}_t$ is positive. The DA test is then calculated as:

$$DA = \frac{SR - SRI}{\sqrt{Var(SR) - Var(SRI)}}, \tag{18}$$

where $Var(SR) = n^{-1}SRI(1-SRI)$ and $Var(SRI) = n^{-1}(2\widehat{P}-1)^2 P(1-P) + n^{-1}(2P-1)^2\widehat{P}(1 - \widehat{P}) + 4n^{-2}P\widehat{P}(1 - P)(1 - \widehat{P})$. A significant DA statistic indicates the model

---

[22]See Alquist and Kilian (2010).

forecast $\hat{h}_t$ has predictive content for the underlying volatility RV_t.

Test of Equal Predictive Ability

It seems natural to rank the models according to the statistical loss functions, which would provide information about the relative forecasting ability of the different models. However, a common finding in the literature is that no unique model dominates the rest for all of the loss functions. A more rigorous comparison is obtained by evaluating the relative predictive accuracy with Diebold and Mariano's (1995) test of equal predictive ability (EPA). The EPA test is a pairwise comparison of two models, where the null hypothesis is that there is no difference in the predictive accuracy of the two forecasts. Building on the Diebold and Mariano framework, West (1996) develops the asymptotic theory for the EPA test; meanwhile Giacomini and White (2006) investigate the finite sample properties of the EPA test.

Suppose $\{\hat{r}_{i,t}\}_{t=1}^{n}$ and $\{\hat{r}_{j,t}\}_{t=1}^{n}$ are two sequences of forecasts of the series $\{\hat{r}_t\}$ generated by two competing models, i and j. Let $\{\hat{e}_{i,t}\}_{t=1}^{n}$ and $\{\hat{e}_{j,t}\}_{t=1}^{n}$ be the corresponding forecast errors. Consider the loss function $g(.)$ and define the difference between the two forecasts as $d_t \equiv [g(\hat{e}_{i,t}) - g(\hat{e}_{j,t})]$, where $g(\hat{e}_{i,t})$ denotes the loss function for the benchmark model i and $g(\hat{e}_{j,t})$ is the loss function for the alternative model j. Giacomini and White (2006) show that if the parameter estimates are constructed using a rolling scheme with a finite observation window, the asymptotic distribution of the sample mean loss differential $\bar{d} = \frac{1}{n} \sum_{t=1}^{n} d_t$ is asymptotically normal as long as $\{d_t\}_{t=1}^{n}$ is covariance stationary with a short memory. So the DM statistic for testing the null hypothesis of equal forecast accuracy between models i and j is simply $DM = \bar{d}/\sqrt{\widehat{V}(\bar{d})}$, where the asymptotic variance $\widehat{V}(\bar{d})$ can be estimated by Newey-West's HAC estimator.[23] DM has a standard normal distribution under H_0. If the test statistic DM is significantly negative, the benchmark

---

[23]$\widehat{V}(\bar{d}) = n^{-1}\left(\hat{\gamma} + 2\sum_{k=1}^{q} \omega_k \hat{\gamma}_k\right)$, where $q = h - 1$, $\omega_k = 1 - \frac{k}{q+1}$ is the lag window and $\hat{\gamma}_i$ is an estimate of the i-th order autocovariance of the series $\{d_t\}$, where $\hat{\gamma}_k = \frac{1}{n}\sum_{t=k+1}^{n}\left(d_t - \bar{d}\right)\left(d_{t-k} - \bar{d}\right)$ for $k = 1, ..., q$.

model is better since it has a smaller loss function; if DM is significantly positive, then the benchmark model is outperformed.

Test of Superior Predictive Ability

In our case when the objective is to evaluate the relative performance of more than two models it is useful to consider White's (2000) Reality Check (RC) test for out-of-sample forecast evaluation. The RC evaluates whether a benchmark forecasting model is significantly outperformed by a set of alternative models given a particular loss function.

Consider comparing $l+1$ forecasting models where model 0 is defined as the benchmark model and $k = 1, ..., l$ denote the l alternative models. Let $L_{t,k} \equiv L(RV_t, \widehat{h}_{t,k})$ denote the loss if a forecast $\widehat{h}_{t,k}$ is made with the k-th model when the realized volatility equals RV_t. Similarly, the loss function of the forecasts from the benchmark model is denoted by $L_{t,0}$. The performance of the k-th forecast model relative to the benchmark is given by

$$f_{t,k} = L_{t,0} - L_{t,k}, \qquad k = 1, ..., l; \qquad t = 1, ..., n.$$

Under the assumption that $f_{t,k}$ is stationary, the expected relative performance of model k to the benchmark can be defined as $\mu_k = E[f_{t,k}]$ for $k = 1, ..., l$. The value of μ_k will be positive for any model k that outperforms the benchmark. Thus, the null hypothesis for testing whether any of the competing models significantly outperform the benchmark may be defined in terms of μ_k for $k = 1, ..., l$ or, more specifically:

$$H_0 : \mu_{\max} \equiv \max_{k=1,...,l} \mu_k \leq 0.$$

The alternative is that the best model has a smaller loss function relative to the benchmark. If the null is rejected, then there is evidence that at least one of the competing models has a significantly smaller loss function than the benchmark. As a result, White's

RC test is constructed from the test statistic

$$T_n^{RC} \equiv \max_{k=1,...,l} n^{\frac{1}{2}} \overline{f}_{n,k},$$

where $\overline{f}_{n,k} = n^{-1} \sum_{t=1}^{n} f_{t,k}$. T_n^{RC}'s asymptotic null distribution is also normal with mean 0 and some long-run variance Ω.

Note that T_n^{RC}'s asymptotic distribution relies on the assumption that $\mu_k = 0$ for all k, however, any negative values of μ_k would also conform with H_0. Hansen (2005) proposes an alternative Super Predictive Ability (SPA) test statistic:

$$T_n^{SPA} = \max_{k} \left(\frac{n^{\frac{1}{2}} \overline{f}_{n,k}}{\sqrt{\widehat{var}(n^{\frac{1}{2}} \overline{f}_{n,k})}}, 0 \right),$$

where $\widehat{var}(n^{\frac{1}{2}} \overline{f}_{n,k})$ is a consistent estimator of the variance of $n^{\frac{1}{2}} \overline{f}_{n,k}$ obtained via bootstrap. The distribution under the null is $N(\hat{\mu}, \Omega)$, where $\hat{\mu}$ is a chosen estimator for μ that conforms with H_0. Since different choices of $\hat{\mu}$ would result in difference p-values, Hansen proposes three estimators $\hat{\mu}^l \leq \hat{\mu}^c \leq \hat{\mu}^u$. We name the resulting tests SPA_l, SPA_c, and SPA_u, respectively. SPA_c would lead to a consistent estimate of the asymptotic distribution of the test statistic. SPA_l uses the lower bound of $\hat{\mu}$ and the p-value is asymptotically smaller than the correct p-value, making it a liberal test. In other words, it is insensitive to the inclusion of poor models. SPA_u uses the upper bound of $\hat{\mu}$ and it is a conservative test instead. It has the same asymptotic distribution as the RC test and is sensitive to the inclusion of poor models.

On a final note, the distinction between Hansen's SPA test and Diebold and Mariano's EPA test simply lies in the null hypothesis. H_0 is a simple hypothesis in EPA whilst it is a composite hypothesis in SPA. In other words, EPA is a pairwise comparison, meanwhile SPA is a groupwise comparison.

Evaluating Relative Out-of-Sample Performance

The volatility forecasts obtained from the EGARCH-GED, EGARCH-t and MS-GARCH-t models for the 1-, 5-, 22-, and 66-day horizons are collected in Figure 3. The corresponding realized volatility is also plotted for reference. At 1- and 5-day horizons, the forecasts the two models yield are very similar. They move closely with the realized volatility and are able to capture the huge spikes and dips in the realized volatility. Similarly, at a 22-day horizon, both models are also able to forecast the major upward and downward movements in the realized volatility of oil futures. Only when we increase the forecast horizon to 66 days, or 3 months, our forecasts contain less information about the aggregated realized volatility during the out-of-sample period, which is as expected.

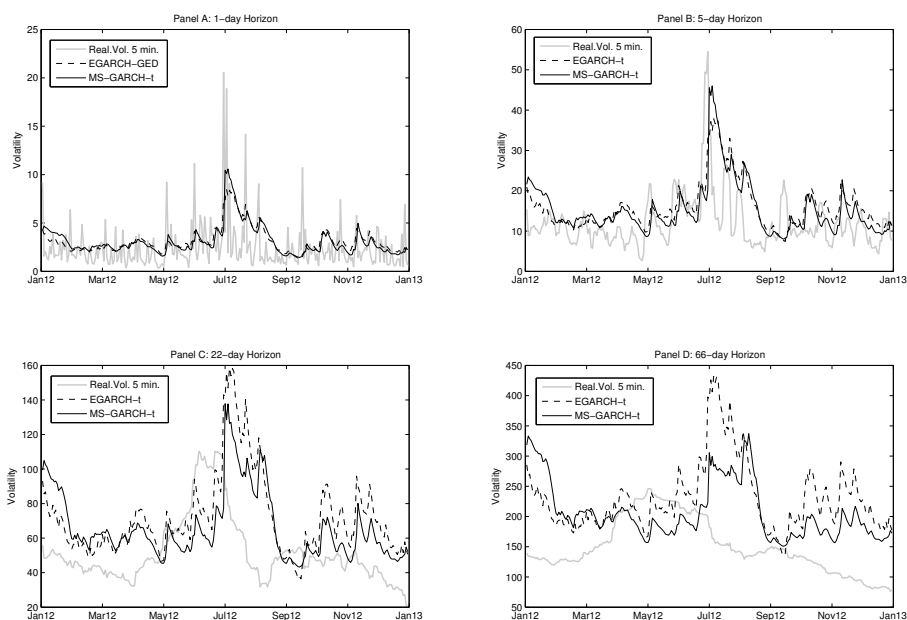Figure 3: Volatility Forecast Comparisons for Select Models. The out-of-sample period extends from January 3, 2012 through Dec 30, 2013.

The estimated loss functions of our out-of-sample forecasts, in addition to the Success Ratio (SR) and the Directional Accuracy (DA) test, are reported in Tables 4 and 5. Recall that our volatility proxy is the realized volatility measure calculated from the 5-minute futures returns.

Out-of-sample evaluation of the one- and five-step-ahead volatility forecasts

1-step-ahead volatility forecasts														
Model	MSE_1	Rank	MSE_2	Rank	$QLIKE$	Rank	R^2LOG	Rank	MAD_1	Rank	MAD_2	Rank	SR	DA
GARCH-N	0.460	10	7.018	10	1.911	10	0.738	9	1.843	10	0.548	9	0.59	0.739
GARCH-*t*	0.450	8	6.708	7	1.904	8	0.749	10	1.843	9	0.553	10	0.57	0.446
GARCH-GED	0.449	7	6.762	8	1.905	9	0.737	8	1.831	7	0.548	8	0.57	0.253
EGARCH-N	0.405	3	5.754	5	1.867	2	0.691	2	1.735	2	**0.519**	1	0.63	2.280*
EGARCH-*t*	0.401	2	5.694	2	1.871	5	0.707	3	1.741	3	0.527	3	0.61	2.379**
EGARCH-GED	**0.396**	1	**5.645**	1	**1.867**	1	**0.691**	1	**1.721**	1	0.519	2	0.59	1.389
GJR-N	0.423	6	5.981	6	1.868	4	0.709	5	1.797	5	0.534	5	0.63	2.569**
GJR-*t*	0.416	5	5.749	4	1.873	6	0.729	6	1.798	6	0.542	6	0.61	2.142*
GJR-GED	0.410	4	5.720	3	1.868	3	0.708	4	1.775	4	0.533	4	0.61	1.973*
MS-GARCH-N	0.927	12	27.592	12	1.967	12	1.072	12	2.794	12	0.717	12	0.61	1.438
MS-GARCH-*t*	0.453	9	6.881	9	1.897	7	0.733	7	1.836	8	0.545	7	0.61	1.872*
MS-GARCH-GED	0.516	11	7.840	11	1.918	11	0.817	11	2.009	11	0.587	11	0.60	1.673*
5-step-ahead volatility forecasts														
Model	MSE_1	Rank	MSE_2	Rank	$QLIKE$	Rank	R^2LOG	Rank	MAD_1	Rank	MAD_2	Rank	SR	DA
GARCH-N	1.184	8	85.883	9	3.521	8	0.329	6	6.386	6	0.829	6	0.63	2.588**
GARCH-*t*	1.103	4	74.115	5	3.517	7	0.323	5	6.162	5	0.814	5	0.61	2.084*
GARCH-GED	1.108	5	76.392	6	3.517	6	0.319	4	6.153	4	0.809	4	0.61	2.084*
EGARCH-N	1.198	9	83.609	8	3.524	10	0.340	9	6.554	9	0.851	9	0.63	2.830**
EGARCH-*t*	**1.020**	1	**63.927**	1	**3.512**	1	0.314	3	**6.014**	1	0.805	3	0.65	3.742**
EGARCH-GED	1.040	2	67.459	2	3.513	2	0.312	2	6.034	2	0.802	2	0.62	2.471**
GJR-N	1.302	10	98.960	10	3.523	9	0.349	10	6.928	10	0.881	10	0.65	3.337**
GJR-*t*	1.121	6	73.059	4	3.516	5	0.333	8	6.453	7	0.851	8	0.64	3.309**
GJR-GED	1.144	7	77.663	7	3.516	4	0.329	7	6.461	8	0.844	7	0.63	2.897**
MS-GARCH-N	4.131	12	610.011	12	3.641	12	0.748	12	13.823	12	1.467	12	0.62	2.231*
MS-GARCH-*t*	1.066	3	72.419	3	3.514	3	**0.309**	1	6.065	3	**0.801**	1	0.63	2.614**
MS-GARCH-GED	1.472	11	109.942	11	3.543	11	0.398	11	7.588	11	0.967	11	0.63	2.856**

Table 4: Note: The volatility proxy is given by the realized volatility calculated with five-minute returns aggregated with the overnight returns. * and ** denote 5% and 1% significance levels for the DA statistic, respectively.

Out-of-sample evaluation of the 22- and 66-step-ahead volatility forecasts

22-step-ahead volatility forecasts														
Model	MSE_1	Rank	MSE_2	Rank	$QLIKE$	Rank	R^2LOG	Rank	MAD_1	Rank	MAD_2	Rank	SR	DA
GARCH-N	5.541	8	1757.638	8	5.027	8	0.324	8	32.255	8	1.945	8	0.64	2.088*
GARCH-*t*	4.602	4	1326.653	4	5.014	4	0.285	4	29.551	4	1.822	5	0.62	1.543
GARCH-GED	4.710	5	1397.245	5	5.015	5	0.287	5	29.647	5	1.818	4	0.62	1.508
EGARCH-N	5.905	9	1915.389	9	5.031	9	0.337	9	32.985	9	1.972	9	0.64	2.445**
EGARCH-*t*	3.699	2	1028.852	2	4.995	2	0.235	2	25.486	2	1.594	2	0.65	3.662**
EGARCH-GED	3.858	3	1115.967	3	4.997	3	0.239	3	25.973	3	1.611	3	0.65	3.000**
GJR-N	6.708	11	2371.000	11	5.041	10	0.365	10	35.648	10	2.089	10	0.67	3.330**
GJR-*t*	4.948	6	1462.159	6	5.019	6	0.301	6	30.688	6	1.875	6	0.65	2.885**
GJR-GED	5.268	7	1626.635	7	5.022	7	0.311	7	31.504	7	1.905	7	0.65	2.653**
MS-GARCH-N	24.116	12	13214.732	12	5.228	12	0.964	12	79.388	12	3.972	12	0.64	2.088*
MS-GARCH-*t*	**3.152**	1	**827.289**	1	**4.988**	1	**0.207**	1	**23.620**	1	**1.501**	1	0.64	2.208*
MS-GARCH-GED	6.381	10	1969.727	10	5.047	11	0.378	11	35.722	11	2.152	11	0.64	2.679**
66-step-ahead volatility forecasts														
Model	MSE_1	Rank	MSE_2	Rank	$QLIKE$	Rank	R^2LOG	Rank	MAD_1	Rank	MAD_2	Rank	SR	DA
GARCH-N	32.161	9	29263.018	9	6.203	9	0.625	9	146.342	9	4.986	9	0.54	-0.460
GARCH-*t*	22.466	4	18344.934	4	6.153	4	0.475	4	114.508	4	4.071	4	0.50	-1.614
GARCH-GED	23.880	5	19971.742	5	6.160	6	0.496	6	118.963	5	4.197	5	0.51	-1.519
EGARCH-N	35.213	10	33789.444	10	6.214	10	0.656	10	156.743	10	5.237	10	0.61	2.229*
EGARCH-*t*	14.429	2	11311.522	2	6.098	2	0.319	2	86.211	2	3.156	2	0.60	2.294*
EGARCH-GED	14.692	3	11772.157	3	6.098	3	0.320	3	86.672	3	3.160	3	0.59	1.886*
GJR-N	38.503	11	38807.487	11	6.227	11	0.699	11	164.276	11	5.435	11	0.56	0.191
GJR-*t*	23.963	6	20310.300	6	6.159	5	0.493	5	120.781	6	4.243	6	0.53	-0.411
GJR-GED	26.506	7	23220.206	7	6.172	7	0.532	7	127.120	7	4.416	7	0.52	-0.969
MS-GARCH-N	104.275	12	138339.793	12	6.469	12	1.500	12	327.635	12	9.476	12	0.55	-0.257
MS-GARCH-*t*	**10.422**	1	**7604.255**	1	**6.072**	1	**0.243**	1	**72.123**	1	**2.720**	1	0.53	-0.493
MS-GARCH-GED	28.3567	8	24032.2875	8	6.1900	8	0.5774	8	139.2564	8	4.8280	8	0.55	0.2461

Table 5: Note: The volatility proxy is given by the realized volatility calculated with five-minute returns aggregated with the overnight returns. * and ** denote 5% and 1% significance levels for the DA statistic, respectively.

At a one-day forecast horizon, five out of the six loss functions rank the EGARCH-GED first. Only the MAD_2 ranks the EGARCH-GED second after the EGARCH-N. Instead, when we consider a 5-day (one-week) horizon the EGARCH-GED is uniformly ranked second, whereas the EGARCH-t is ranked first according to four of the criteria, and the MS-GARCH-t is ranked first by the R^2LOG and the MAD_2. At longer horizons such as 22 and 66 days (one and three months, respectively), evidence in favor of a switching model is overwhelming: the MS-GARCH-t is ranked first by all loss functions.

The SR averages over 50% for all models and forecast horizons, indicating that all models forecast the direction of the change correctly in more that 50% of the sample. For the 5- and 22-day forecast horizons, the SR exceeds 60% for all models (averages 63% and 64%, respectively), whereas for the 1-day forecast horizon the SR ranges between 57% and 59% for four of the competing models, and equals or exceeds 60% for the remaining eight models. In addition, at a longer 66-day horizon the SR averages 55% across all models, suggesting the direction of the change is more difficult to predict for this longer 3-month horizon. The results of the DA test are consistent with this finding. Recall that a significant DA statistic indicates that the model forecasts have predictive content for the underlying volatility. In particular, the DA test is significant at the 1% level for a majority of the models at 5- and 22-day forecast horizons. At the shorter 1-day horizon seven of the models exhibit a statistically significant DA at the 5% level. In contrast, for the 3-month forecast horizon only the three EGARCH models have a DA statistic that is significant at a 5% level.

Tables 6-9 report the selected DM test statistics with GARCH-t, EGARCH-GED, EGARCH-t, and MS-GARCH-t as benchmark models.[24] These test results are in line with the rankings reported in Table 1.4. Consider first the one-day-ahead forecast where the EGARCH-GED was ranked higher by most of the loss functions. As Table 1.5b shows,

---

[24]The complete list of all DM test statistics can be requested from the authors.

we reject the null of equal predictive ability at a 5% level for three of the eleven competing models under all six loss functions and three extra models under five loss functions, favoring the benchmark model. In addition, relative to the EGARCH-t and GJR-t models, the EGARCH-GED yields a more accurate forecast according to some of the loss functions. Note also that when an alternative model is used as the benchmark (see Tables 1.5a, 1.5c and 5d), we also find statistical evidence that the EGARCH-GED generates the smaller forecast errors in the majority of the cases.

Diebold and Mariano test - GARCH-t Benchmark

Panel A: One day Horizon						Panel B: Five day Horizon					
Model	MSE1	MSE2	QLIKE	R2LOG	MAD1	MAD2	Model	MSE1	MSE2	QLIKE	R2LOG	MAD1	MAD2
GARCH-N	-0.74	-1.32	-0.95	0.70	0.65	-0.01	GARCH-N	-1.16	-1.31	-0.94	-0.49	-0.71	-1.01
GARCH-GED	0.29	-0.77	-0.31	1.89	1.72	1.10	GARCH-GED	-0.25	-0.89	0.08	0.78	0.68	0.12
EGARCH-N	2.44+	1.78	3.18++	2.38+	3.32++	2.94++	EGARCH-N	-1.16	-1.19	-0.62	-0.81	-1.12	-1.41
EGARCH-t	2.74++	2.51+	3.28++	2.10+	2.84++	2.84++	EGARCH-t	1.12	1.34	0.54	0.55	0.34	0.60
EGARCH-GED	3.23++	2.43+	3.65++	2.97++	3.97++	3.90++	EGARCH-GED	1.00	1.18	0.38	0.63	0.49	0.61
GJR-N	1.29	1.07	2.93++	1.97+	1.99+	1.05	GJR-N	-1.72	-1.55	-0.96	-1.49	-2.19*	-2.16*
GJR-t	2.07+	1.82	2.61++	1.51	1.85	1.81	GJR-t	-0.40	0.21	0.11	-1.10	-2.06*	-1.86
GJR-GED	2.51+	1.74	3.16++	3.19++	3.50++	2.81++	GJR-GED	-0.91	-0.77	0.19	-0.68	-1.7	-1.87
MS-GARCH-N	-2.69**	-1.81	-2.89**	-3.93**	-4.02**	-3.19**	MS-GARCH-N	-3.32**	-2.25*	-4.64**	-4.54**	-4.80**	-3.90**
MS-GARCH-t	-0.18	-0.73	0.83	0.60	0.60	0.15	MS-GARCH-t	0.54	0.38	0.30	0.73	0.35	0.32
MS-GARCH-GED	-2.65**	-2.09*	-1.33	-2.35*	-2.49*	-2.82**	MS-GARCH-GED	-3.19**	-2.16*	-3.24**	-3.61**	-4.01**	-3.70**

Panel C: Twenty-two day Horizon						Panel D: Sixty-six day Horizon					
Model	MSE1	MSE2	QLIKE	R2LOG	MAD1	MAD2	Model	MSE1	MSE2	QLIKE	R2LOG	MAD1	MAD2
GARCH-N	-2.45*	-1.86	-3.43**	-3.39**	-2.76**	-2.44*	GARCH-N	-5.20**	-3.60**	-8.42**	-7.20**	-11.50**	-8.47**
GARCH-GED	-1.04	-1.24	-0.35	-0.49	0.26	-0.29	GARCH-GED	-3.43**	-2.64**	-4.80**	-4.43**	-5.51**	-4.56**
EGARCH-N	-2.39*	-2.11*	-2.10*	-2.31*	-1.70	-1.91	EGARCH-N	-4.36**	-3.45**	-5.67**	-5.29**	-6.07**	-5.59**
EGARCH-t	3.62++	2.85++	3.69++	3.59++	4.25++	4.32++	EGARCH-t	5.93++	5.60++	5.81++	5.53++	5.93++	6.28++
EGARCH-GED	3.48++	3.44++	3.03++	3.07++	3.61++	3.90++	EGARCH-GED	5.72++	5.95++	5.42++	5.22++	5.42++	5.76++
GJR-N	-2.46*	-1.90	-3.15**	-3.20**	-2.83**	-2.53*	GJR-N	-3.93**	-2.81**	-6.38**	-5.59**	-7.29**	-5.65**
GJR-t	-2.13*	-2.19*	-1.47	-1.89	-1.47	-1.70	GJR-t	-1.95	-2.09*	-1.75	-1.54	-2.62**	-2.66**
GJR-GED	-2.45*	-2.16*	-2.16*	-2.47*	-1.89	-2.06*	GJR-GED	-3.28**	-2.72**	-3.97**	-3.81**	-4.32**	-3.88**
MS-GARCH-N	-4.18**	-2.94**	-6.59**	-5.87**	-6.73**	-5.25**	MS-GARCH-N	-7.28**	-4.92**	-13.02**	-10.03**	-18.95**	-12.17**
MS-GARCH-t	2.20+	1.93	2.03+	2.36+	2.20+	2.21+	MS-GARCH-t	3.68++	3.21++	3.88++	3.86++	3.94++	3.89++
MS-GARCH-GED	-4.19**	-2.83**	-4.11**	-4.66**	-3.51**	-3.64**	MS-GARCH-GED	-6.74**	-6.23**	-6.64**	-6.61**	-7.56**	-7.77**

Table 6: Note: * and ** represent the DM test statistic for which the null hypothesis of equal predictive accuracy can be rejected at 5% and 1%, respectively and the DM statistic is negative. + and ++ represent the 5% and 1% significance level when the DM test statistic is positive.

Regarding the 5-day horizon (1 week), there is little statistical difference in the forecast accuracy comparison between the benchmark models and any of the non-switching models. The MS-GARCH-t is found to have equal accuracy as the benchmark models as well. In contrast, as the forecast horizon increases to 22 and 66 days (1 and 3 months), statistical evidence that the forecast accuracy differences are negative, in favor of switching models, especially for the MS-GARCH-t, is prevalent.

RC and SPA tests are reported in Tables 10 and 11, where each model is compared against all the others. Recall that the null hypothesis is that there are no other models

Diebold and Mariano test - EGARCH-GED Benchmark

	Panel A: One day Horizon							Panel B: Five day Horizon					
Model	MSE1	MSE2	QLIKE	R2LOG	MAD1	MAD2	Model	MSE1	MSE2	QLIKE	R2LOG	MAD1	MAD2
GARCH-N	-2.60**	-2.35*	-3.17**	-1.95	-2.62**	-2.61**	GARCH-N	-1.38	-1.41	-0.91	-0.92	-0.81	-1.02
GARCH-t	-3.23**	-2.43*	-3.65**	-2.97**	-3.97**	-3.90**	GARCH-t	-1.00	-1.18	-0.38	-0.63	-0.49	-0.61
GARCH-GED	-2.83**	-2.38*	-3.36**	-2.30*	-3.30**	-3.23**	GARCH-GED	-0.97	-1.21	-0.38	-0.42	-0.27	-0.49
EGARCH-N	-0.85	-0.47	-0.06	-0.06	0.09	-0.50	EGARCH-N	-2.28*	-1.82	-2.94**	-2.68**	-2.72**	-2.44*
EGARCH-t	-0.83	-0.41	-1.54	-2.20*	-2.13*	-1.36	EGARCH-t	0.67	1.10	0.36	-0.25	-0.34	0.20
GJR-N	-1.19	-0.70	-0.13	-0.74	-1.28	-1.45	GJR-N	-1.85	-1.64	-1.16	-1.65	-2.14*	-2.08*
GJR-t	-1.73	-0.65	-0.83	-2.00*	-2.66**	-2.65**	GJR-t	-1.55	-1.96	-0.34	-1.19	-2.05*	-2.29*
GJR-GED	-1.10	-0.34	-0.13	-0.94	-1.71	-1.80	GJR-GED	-1.68	-1.92	-0.33	-1.02	-1.69	-1.98*
MS-GARCH-N	-2.84**	-1.85	-4.44**	-4.22**	-4.39**	-3.40**	MS-GARCH-N	-3.28**	-2.24*	-4.21**	-4.32**	-4.59**	-3.80**
MS-GARCH-t	-2.36*	-2.09*	-2.88**	-1.69	-2.08*	-2.28*	MS-GARCH-t	-0.31	-0.67	-0.14	0.20	0.00	-0.10
MS-GARCH-GED	-3.56**	-2.49*	-4.57**	-4.42**	-4.51**	-4.06**	MS-GARCH-GED	-3.08**	-2.06*	-3.85**	-4.34**	-4.25**	-3.45**

	Panel C: Twenty-two day Horizon							Panel D: Sixty-six day Horizon					
Model	MSE1	MSE2	QLIKE	R2LOG	MAD1	MAD2	Model	MSE1	MSE2	QLIKE	R2LOG	MAD1	MAD2
GARCH-N	-3.49**	-2.36*	-4.37**	-4.37**	-4.73**	-4.33**	GARCH-N	-6.48**	-4.74**	-7.61**	-6.95**	-9.99**	-9.86**
GARCH-t	-3.48**	-3.44**	-3.03**	-3.07**	-3.61**	-3.90**	GARCH-t	-5.72**	-5.95**	-5.42**	-5.22**	-5.42**	-5.76**
GARCH-GED	-3.35**	-2.69**	-3.10**	-3.16**	-3.56**	-3.80**	GARCH-GED	-6.00**	-5.52**	-5.86**	-5.59**	-6.24**	-6.65**
EGARCH-N	-3.74**	-2.63**	-5.22**	-5.21**	-5.13**	-4.37**	EGARCH-N	-6.31**	-4.49**	-8.90**	-7.87**	-12.35**	-10.26**
EGARCH-t	1.30	1.44	0.97	0.83	0.69	0.98	EGARCH-t	0.84	1.15	0.19	0.28	0.14	0.46
GJR-N	-3.12**	-2.15*	-4.63**	-4.60**	-4.61**	-3.80**	GJR-N	-5.35**	-3.51**	-8.39**	-7.41**	-10.71**	-8.48**
GJR-t	-4.50**	-3.73**	-3.97**	-4.41**	-4.23**	-4.53**	GJR-t	-7.09**	-5.87**	-7.24**	-6.97**	-7.74**	-8.24**
GJR-GED	-3.90**	-2.91**	-4.00**	-4.25**	-4.26**	-4.27**	GJR-GED	-6.11**	-4.79**	-6.77**	-6.36**	-7.77**	-7.81**
MS-GARCH-N	-4.28**	-2.97**	-6.77**	-6.06**	-7.15**	-5.54**	MS-GARCH-N	-7.61**	-5.09**	-12.28**	-9.85**	-20.74**	-13.66**
MS-GARCH-t	1.18	1.25	0.80	1.12	0.81	0.94	MS-GARCH-t	1.64	1.53	1.67	1.76	1.58	1.58
MS-GARCH-GED	-5.17**	-3.24**	-5.55**	-6.04**	-5.21**	-5.30**	MS-GARCH-GED	-8.00**	-8.03**	-7.46**	-7.13**	-9.09**	-10.08**

Table 7: Note: * and ** represent the DM test statistic for which the null hypothesis of equal predictive accuracy can be rejected at 5% and 1%, respectively and the DM statistic is negative. + and ++ represent the 5% and 1% significance level when the DM test statistic is positive.

Diebold and Mariano test - EGARCH-t Benchmark

	Panel A: One day Horizon							Panel B: Five day Horizon					
Model	MSE1	MSE2	QLIKE	R2LOG	MAD1	MAD2	Model	MSE1	MSE2	QLIKE	R2LOG	MAD1	MAD2
GARCH-N	-2.13*	-2.26*	-2.70**	-1.11	-1.59	-1.81	GARCH-N	-1.28	-1.38	-0.98	-0.71	-0.60	-0.89
GARCH-t	-2.74**	-2.51*	-3.28**	-2.10*	-2.84**	-2.84**	GARCH-t	-1.12	-1.34	-0.54	-0.55	-0.34	-0.60
GARCH-GED	-2.31*	-2.38*	-2.90**	-1.36	-2.07*	-2.18*	GARCH-GED	-1.00	-1.27	-0.52	-0.30	-0.13	-0.47
EGARCH-N	-0.27	-0.17	0.62	0.82	0.86	0.15	EGARCH-N	-1.81	-1.63	-1.89	-1.63	-1.68	-1.75
EGARCH-GED	0.83	0.41	1.54	2.20+	2.13+	1.36	EGARCH-GED	-0.67	-1.10	-0.36	0.25	0.34	-0.2
GJR-N	-0.81	-0.48	0.35	-0.07	-0.50	-0.88	GJR-N	-1.69	-1.57	-1.26	-1.38	-1.73	-1.79
GJR-t	-1.20	-0.22	-0.35	-1.22	-1.81	-1.88	GJR-t	-1.75	-1.91	-0.57	-1.21	-1.96	-2.18*
GJR-GED	-0.56	-0.08	0.46	-0.07	-0.68	-0.92	GJR-GED	-1.55	-1.69	-0.52	-0.88	-1.38	-1.65
MS-GARCH-N	-2.79**	-1.85	-4.26**	-3.93**	-4.10**	-3.27**	MS-GARCH-N	-3.24**	-2.24*	-4.28**	-4.26**	-4.46**	-3.70**
MS-GARCH-t	-2.01*	-2.11*	-2.35*	-0.91	-1.33	-1.72	MS-GARCH-t	-0.52	-0.99	-0.26	0.26	0.09	-0.15
MS-GARCH-GED	-3.15**	-2.46*	-3.81**	-3.27**	-3.51**	-3.38**	MS-GARCH-GED	-2.76**	-1.97*	-3.76**	-3.65**	-3.70**	-3.06**

	Panel C: Twenty-two day Horizon							Panel D: Sixty-six day Horizon					
Model	MSE1	MSE2	QLIKE	R2LOG	MAD1	MAD2	Model	MSE1	MSE2	QLIKE	R2LOG	MAD1	MAD2
GARCH-N	-3.19**	-2.22*	-4.54**	-4.34**	-4.73**	-3.96**	GARCH-N	-6.19**	-4.45**	-7.71**	-6.97**	-10.26**	-9.60**
GARCH-t	-3.62**	-2.85**	-3.69**	-3.59**	-4.25**	-4.32**	GARCH-t	-5.93**	-5.60**	-5.81**	-5.53**	-5.93**	-6.28**
GARCH-GED	-3.12**	-2.34*	-3.52**	-3.44**	-3.86**	-3.72**	GARCH-GED	-5.91**	-4.97**	-6.16**	-5.80**	-6.70**	-6.97**
EGARCH-N	-3.41**	-2.46*	-5.10**	-4.85**	-4.92**	-3.98**	EGARCH-N	-5.99**	-4.27**	-8.71**	-7.66**	-11.96**	-9.62**
EGARCH-GED	-1.30	-1.44	-0.97	-0.83	-0.69	-0.98	EGARCH-GED	-0.84	-1.15	-0.19	-0.28	-0.14	-0.46
GJR-N	-2.96**	-2.10*	-4.58**	-4.39**	-4.47**	-3.56**	GJR-N	-5.13**	-3.40**	-8.22**	-7.21**	-10.45**	-8.06**
GJR-t	-4.23**	-3.07**	-4.83**	-4.93**	-5.06**	-4.83**	GJR-t	-6.69**	-5.13**	-7.59**	-7.17**	-8.39**	-8.51**
GJR-GED	-3.55**	-2.60**	-4.35**	-4.34**	-4.49**	-4.05**	GJR-GED	-5.79**	-4.39**	-6.89**	-6.39**	-8.09**	-7.73**
MS-GARCH-N	-4.25**	-2.96**	-6.83**	-6.05**	-7.15**	-5.47**	MS-GARCH-N	-7.52**	-5.05**	-12.28**	-9.82**	-20.35**	-13.30**
MS-GARCH-t	1.02	1.07	0.66	1.03	0.70	0.78	MS-GARCH-t	1.67	1.54	1.72	1.81	1.62	1.62
MS-GARCH-GED	-4.88**	-3.00**	-6.17**	-6.37**	-5.88**	-5.56**	MS-GARCH-GED	-8.17**	-7.48**	-7.89**	-7.48**	-9.82**	-10.85**

Table 8: Note: * and ** represent the DM test statistic for which the null hypothesis of equal predictive accuracy can be rejected at 5% and 1%, respectively and the DM statistic is negative. + and ++ represent the 5% and 1% significance level when the DM test statistic is positive.

Diebold and Mariano test - MS-GARCH-t Benchmark

			Panel A: One day Horizon							Panel B: Five day Horizon			
Model	MSE1	MSE2	QLIKE	R2LOG	MAD1	MAD2	Model	MSE1	MSE2	QLIKE	R2LOG	MAD1	MAD2
GARCH-N	-0.38	-0.60	-1.39	-0.20	-0.21	-0.15	GARCH-N	-1.13	-1.26	-0.85	-0.92	-0.65	-0.84
GARCH-t	0.18	0.73	-0.83	-0.60	-0.6	-0.15	GARCH-t	-0.54	-0.38	-0.30	-0.73	-0.35	-0.32
GARCH-GED	0.26	0.55	-0.94	-0.17	-0.22	0.12	GARCH-GED	-0.56	-0.72	-0.29	-0.53	-0.20	-0.28
EGARCH-N	2.07+	1.71	2.77++	1.78	2.09+	2.00+	EGARCH-N	-1.24	-1.09	-0.92	-1.36	-1.16	-1.24
EGARCH-t	2.01+	2.11+	2.35+	0.91	1.33	1.72	EGARCH-t	0.52	0.99	0.26	-0.26	-0.09	0.15
EGARCH-GED	2.36+	2.09+	2.88++	1.69	2.08+	2.28+	EGARCH-GED	0.31	0.67	0.14	-0.20	0.00	0.10
GJR-N	1.20	1.18	2.21+	0.89	0.75	0.64	GJR-N	-1.63	-1.51	-0.90	-1.57	-1.61	-1.75
GJR-t	1.39	1.65	1.67	0.12	0.20	0.65	GJR-t	-0.63	-0.09	-0.17	-1.07	-1.14	-1.06
GJR-GED	1.70	1.62	2.17+	0.88	0.82	1.08	GJR-GED	-0.86	-0.70	-0.15	-0.93	-0.98	-1.06
MS-GARCH-N	-2.83**	-1.82	-3.26**	-4.20**	-4.28**	-3.40**	MS-GARCH-N	-3.38**	-2.27*	-4.37**	-4.58**	-4.60**	-3.91**
MS-GARCH-GED	-3.28**	-2.46*	-3.12**	-3.92**	-3.59**	-3.39**	MS-GARCH-GED	-3.17**	-2.18*	-3.77**	-4.18**	-4.40**	-3.82**

			Panel C: Twenty-two day Horizon							Panel D: Sixty-six day Horizon			
Model	MSE1	MSE2	QLIKE	R2LOG	MAD1	MAD2	Model	MSE1	MSE2	QLIKE	R2LOG	MAD1	MAD2
GARCH-N	-2.44*	-1.97*	-2.53*	-2.84**	-2.53*	-2.46*	GARCH-N	-4.45**	-3.52**	-5.14**	-4.94**	-5.80**	-5.47**
GARCH-t	-2.20*	-1.93	-2.03*	-2.36*	-2.20*	-2.21*	GARCH-t	-3.68**	-3.21**	-3.88**	-3.86**	-3.94**	-3.89**
GARCH-GED	-2.12*	-1.85	-1.99*	-2.29*	-2.07*	-2.09*	GARCH-GED	-3.73**	-3.18**	-4.01**	-3.97**	-4.15**	-4.06**
EGARCH-N	-2.54*	-2.10*	-2.61**	-2.98**	-2.51*	-2.45*	EGARCH-N	-4.52**	-3.56**	-5.52**	-5.26**	-6.29**	-5.72**
EGARCH-t	-1.02	-1.07	-0.66	-1.03	-0.70	-0.78	EGARCH-t	-1.67	-1.54	-1.72	-1.81	-1.62	-1.62
EGARCH-GED	-1.18	-1.25	-0.80	-1.12	-0.81	-0.94	EGARCH-GED	-1.64	-1.53	-1.67	-1.76	-1.58	-1.58
GJR-N	-2.55*	-1.99*	-2.86**	-3.17**	-2.82**	-2.65**	GJR-N	-4.22**	-3.09**	-5.55**	-5.25**	-6.16**	-5.42**
GJR-t	-2.41*	-2.10*	-2.19*	-2.65**	-2.31*	-2.34*	GJR-t	-3.87**	-3.24**	-4.28**	-4.23**	-4.46**	-4.30**
GJR-GED	-2.42*	-2.09*	-2.26*	-2.65**	-2.32*	-2.34*	GJR-GED	-3.85**	-3.20**	-4.26**	-4.20**	-4.46**	-4.28**
MS-GARCH-N	-4.13**	-2.95**	-5.83**	-5.60**	-6.02**	-5.02**	MS-GARCH-N	-7.00**	-4.91**	-9.96**	-8.58**	-13.77**	-10.78**
MS-GARCH-GED	-3.65**	-2.61**	-3.84**	-4.49**	-3.77**	-3.65**	MS-GARCH-GED	-5.46**	-4.67**	-5.75**	-5.56**	-6.70**	-6.69**

Table 9: Note: * and ** represent the DM test statistic for which the null hypothesis of equal predictive accuracy can be rejected at 5% and 1%, respectively and the DM statistic is negative. + and ++ represent the 5% and 1% significance level when the DM test statistic is positive.

that outperform the benchmark. The model in each row is the benchmark model under consideration. To economize space, the tables report the p-values only. The RC, SPA_c, and SPA_l correspond to the Reality Check p-value, Hansen's (2005) consistent, and lower p-values, respectively.[25] For the 1- and 5-day horizons, all three EGARCH models fail to reject the null regardless of the loss function, implying the EGARCH models outperform the other models. Meanwhile, the MS-GARCH-t also outperforms other models at the 5-day horizon, but not at the 1-day horizon (see Table 10). Yet, consistent with the out-of-sample evaluation and the Diebold and Mariano's EPA test results, as the forecast horizon increases we fail to reject the null, not only for some of the EGARCH models, but also for the MS-GARCH-t.

It is interesting to consider here how our results differ from Fong and See (2002) and Nomikos and Pouliasis (2011), who find some evidence that MS-GARCH models are preferred over GARCH models for forecasting the volatility of oil futures. Recall that

---

[25]The p-values are calculated using the stationary bootstrap from Politis and Romano (1994). The number of bootstrap re-samples B is 3000 and the block length q is 2.

Reality Check and Superior Predictive Ability Tests

| | | Horizon: One day | | | | | | | | Horizon: Five days | | | | | |
		MSE1	MSE2	QLIKE	R2LOG	MAD1	MAD2			MSE1	MSE2	QLIKE	R2LOG	MAD1	MAD2
GARCH-N	*SPAl*	0.005	0.047	0.011	0.018	0.005	0.006	GARCH-N	*SPAl*	0.021	0.016	0.056	0.115	0.218	0.145
	SPAc	0.378	0.511	0.011	0.018	0.005	0.006		*SPAc*	0.423	0.498	0.056	0.115	0.247	0.163
	RC	0.378	0.511	0.019	0.237	0.164	0.325		RC	0.423	0.498	0.138	0.397	0.511	0.520
GARCH-*t*	*SPAl*	0.018	0.093	0.007	0.001	0.000	0.006	GARCH-*t*	*SPAl*	0.045	0.073	0.072	0.054	0.127	0.147
	SPAc	0.399	0.574	0.007	0.001	0.000	0.006		*SPAc*	0.472	0.555	0.072	0.054	0.127	0.154
	RC	0.399	0.574	0.021	0.162	0.121	0.339		RC	0.482	0.586	0.197	0.352	0.389	0.535
GARCH-GED	*SPAl*	0.015	0.094	0.011	0.010	0.002	0.007	GARCH-GED	*SPAl*	0.047	0.050	0.087	0.150	0.228	0.189
	SPAc	0.412	0.56	0.011	0.010	0.002	0.007		*SPAc*	0.471	0.536	0.087	0.154	0.281	0.224
	RC	0.412	0.560	0.024	0.232	0.169	0.356		RC	0.478	0.558	0.199	0.456	0.552	0.611
EGARCH-N	*SPAl*	0.238	0.522	0.68	0.503	0.501	0.249	EGARCH-N	*SPAl*	0.104	0.077	0.325	0.316	0.342	0.296
	SPAc	0.650	0.730	0.719	0.613	0.826	0.568		*SPAc*	0.586	0.576	0.325	0.466	0.640	0.55
	RC	0.785	0.898	0.933	0.927	0.949	0.860		RC	0.621	0.609	0.660	0.701	0.828	0.798
EGARCH-*t*	*SPAl*	0.244	0.411	0.381	0.185	0.103	0.234	EGARCH-*t*	*SPAl*	0.44	0.493	0.577	0.317	0.340	0.306
	SPAc	0.807	0.814	0.417	0.283	0.303	0.491		*SPAc*	0.872	0.957	0.800	0.544	0.53	0.639
	RC	0.836	0.913	0.832	0.606	0.612	0.745		RC	0.892	0.961	0.885	0.733	0.756	0.838
EGARCH-GED	*SPAl*	0.806	0.933	0.756	0.544	0.450	0.764	EGARCH-GED	*SPAl*	0.517	0.321	0.691	0.916	0.882	0.822
	SPAc	1.000	1.000	0.980	0.991	0.911	1.000		*SPAc*	0.995	0.944	1.000	1.000	1.000	1.000
	RC	1.000	1.000	0.999	0.999	0.977	1.000		RC	0.997	0.958	1.000	1.000	1.000	1.000
GJR-N	*SPAl*	0.085	0.279	0.656	0.172	0.041	0.038	GJR-N	*SPAl*	0.040	0.047	0.378	0.162	0.213	0.152
	SPAc	0.547	0.670	0.697	0.270	0.083	0.058		*SPAc*	0.458	0.522	0.385	0.185	0.232	0.152
	RC	0.576	0.690	0.918	0.652	0.413	0.465		RC	0.458	0.522	0.795	0.531	0.506	0.501
GJR-*t*	*SPAl*	0.044	0.618	0.236	0.027	0.007	0.008	GJR-*t*	*SPAl*	0.064	0.087	0.396	0.102	0.106	0.111
	SPAc	0.517	0.861	0.236	0.046	0.017	0.008		*SPAc*	0.561	0.569	0.430	0.108	0.106	0.162
	RC	0.612	0.903	0.676	0.313	0.238	0.433		RC	0.619	0.787	0.808	0.422	0.385	0.546
GJR-GED	*SPAl*	0.123	0.652	0.637	0.130	0.016	0.014	GJR-GED	*SPAl*	0.081	0.094	0.527	0.274	0.231	0.187
	SPAc	0.609	0.911	0.645	0.130	0.046	0.020		*SPAc*	0.585	0.619	0.830	0.307	0.356	0.391
	RC	0.723	0.939	0.964	0.624	0.409	0.510		RC	0.653	0.705	0.975	0.696	0.636	0.689
MS-GARCH-N	*SPAl*	0.002	0.040	0.000	0.000	0.000	0.000	MS-GARCH-N	*SPAl*	0.001	0.019	0.000	0.000	0.000	0.000
	SPAc	0.002	0.040	0.000	0.000	0.000	0.000		*SPAc*	0.001	0.019	0.000	0.000	0.000	0.000
	RC	0.002	0.040	0.000	0.000	0.000	0.000		RC	0.001	0.019	0.000	0.000	0.000	0.000
MS-GARCH-*t*	*SPAl*	0.019	0.074	0.020	0.039	0.015	0.014	MS-GARCH-*t*	*SPAl*	0.060	0.046	0.144	0.264	0.201	0.161
	SPAc	0.019	0.074	0.020	0.041	0.016	0.014		*SPAc*	0.088	0.077	0.159	0.345	0.22	0.186
	RC	0.394	0.558	0.053	0.275	0.196	0.341		RC	0.511	0.559	0.309	0.606	0.453	0.514
MS-GARCH-GED	*SPAl*	0.000	0.014	0.000	0.000	0.000	0.000	MS-GARCH-GED	*SPAl*	0.000	0.000	0.000	0.000	0.000	0.000
	SPAc	0.000	0.014	0.000	0.000	0.000	0.000		*SPAc*	0.000	0.000	0.000	0.000	0.000	0.000
	RC	0.216	0.493	0.001	0.007	0.003	0.085		RC	0.247	0.433	0.007	0.030	0.013	0.13

Table 10: Note: This table presents the *p*-values of White's (2000) Reality Check test, and Hansen's (2005) Superior Predictive Ability test. The *SPAl* and *SPAc* are the lower and consistent *p*-values from Hansen (2005), respectively. RC is the *p*-value from White's (2000) Reality Check test. Each row contains the benchmark model. The null hypothesis is that none of the alternative models outperform the benchmark. The *p*-values are calculated using 3000 bootstrap replications with a block length of 2.

Reality Check and Superior Predictive Ability Tests

		Horizon: Twenty-two days								Horizon: Sixty-six days					
				Loss Function								Loss Function				
Benchmark		MSE1	MSE2	QLIKE	R2LOG	MAD1	MAD2	Benchmark		MSE1	MSE2	QLIKE	R2LOG	MAD1	MAD2
	SPAl	0.016	0.014	0.127	0.167	0.118	0.064		*SPAl*	0.018	0.010	0.183	0.118	0.230	0.096
GARCH-N	*SPAc*	0.016	0.512	0.127	0.184	0.125	0.064	GARCH-N	*SPAc*	0.018	0.507	0.210	0.146	0.283	0.117
	RC	0.437	0.513	0.301	0.507	0.412	0.435		RC	0.448	0.507	0.421	0.480	0.568	0.493
	SPAl	0.075	0.055	0.296	0.213	0.192	0.224		*SPAl*	0.081	0.044	0.404	0.206	0.450	0.336
GARCH-*t*	*SPAc*	0.115	0.569	0.328	0.267	0.258	0.34	GARCH-*t*	*SPAc*	0.150	0.580	0.461	0.292	0.596	0.500
	RC	0.564	0.607	0.529	0.59	0.554	0.637		RC	0.562	0.609	0.667	0.604	0.776	0.737
	SPAl	0.07	0.027	0.286	0.355	0.289	0.239		*SPAl*	0.085	0.024	0.418	0.334	0.553	0.363
GARCH-GED	*SPAc*	0.100	0.535	0.319	0.451	0.382	0.336	GARCH-GED	*SPAc*	0.142	0.557	0.463	0.442	0.725	0.504
	RC	0.552	0.555	0.514	0.700	0.639	0.662		RC	0.580	0.576	0.661	0.715	0.848	0.770
	SPAl	0.025	0.025	0.206	0.132	0.126	0.068		*SPAl*	0.010	0.010	0.128	0.037	0.059	0.027
EGARCH-N	*SPAc*	0.026	0.524	0.216	0.135	0.131	0.072	EGARCH-N	*SPAc*	0.010	0.500	0.128	0.037	0.059	0.027
	RC	0.475	0.525	0.385	0.445	0.426	0.452		RC	0.439	0.500	0.323	0.345	0.327	0.373
	SPAl	0.585	0.541	0.804	0.559	0.337	0.415		*SPAl*	0.663	0.589	0.827	0.428	0.678	0.702
EGARCH-*t*	*SPAc*	0.935	0.989	0.948	0.781	0.663	0.730	EGARCH-*t*	*SPAc*	0.950	0.985	0.974	0.675	0.819	0.892
	RC	0.961	0.991	0.970	0.853	0.785	0.874		RC	0.968	0.990	0.982	0.788	0.876	0.917
	SPAl	0.281	0.071	0.570	0.693	0.741	0.637		*SPAl*	0.311	0.085	0.564	0.468	0.709	0.655
EGARCH-GED	*SPAc*	0.805	0.728	0.918	0.997	1.000	0.999	EGARCH-GED	*SPAc*	0.668	0.673	0.875	0.800	0.979	0.863
	RC	0.902	0.821	0.951	0.997	1.000	0.999		RC	0.870	0.775	0.908	0.872	0.982	0.954
	SPAl	0.006	0.009	0.218	0.032	0.014	0.010		*SPAl*	0.005	0.007	0.092	0.008	0.003	0.003
GJR-N	*SPAc*	0.006	0.471	0.238	0.032	0.014	0.010	GJR-N	*SPAc*	0.005	0.471	0.092	0.008	0.003	0.003
	RC	0.391	0.471	0.500	0.337	0.212	0.278		RC	0.370	0.471	0.332	0.268	0.141	0.233
	SPAl	0.068	0.019	0.499	0.142	0.057	0.057		*SPAl*	0.035	0.028	0.462	0.056	0.033	0.031
GJR-*t*	*SPAc*	0.154	0.615	0.650	0.161	0.059	0.096	GJR-*t*	*SPAc*	0.091	0.572	0.515	0.073	0.033	0.036
	RC	0.564	0.654	0.835	0.503	0.340	0.453		RC	0.530	0.591	0.766	0.396	0.304	0.412
	SPAl	0.046	0.024	0.551	0.217	0.104	0.078		*SPAl*	0.023	0.011	0.506	0.085	0.058	0.030
GJR-GED	*SPAc*	0.053	0.541	0.765	0.276	0.106	0.093	GJR-GED	*SPAc*	0.027	0.528	0.581	0.085	0.060	0.031
	RC	0.523	0.552	0.904	0.612	0.435	0.482		RC	0.472	0.535	0.835	0.462	0.365	0.414
	SPAl	0.000	0.014	0.000	0.000	0.000	0.000		*SPAl*	0.000	0.005	0.000	0.000	0.000	0.000
MS-GARCH-N	*SPAc*	0.000	0.014	0.000	0.000	0.000	0.000	MS-GARCH-N	*SPAc*	0.000	0.005	0.000	0.000	0.000	0.000
	RC	0.000	0.014	0.000	0.000	0.000	0.000		RC	0.000	0.005	0.000	0.000	0.000	0.000
	SPAl	0.143	0.079	0.398	0.543	0.342	0.263		*SPAl*	0.231	0.102	0.521	0.577	0.595	0.496
MS-GARCH-*t*	*SPAc*	0.331	0.110	0.540	0.797	0.539	0.469	MS-GARCH-*t*	*SPAc*	0.395	0.194	0.691	0.839	0.810	0.643
	RC	0.671	0.625	0.667	0.880	0.694	0.695		RC	0.748	0.663	0.779	0.918	0.862	0.842
	SPAl	0.000	0.002	0.000	0.000	0.000	0.000		*SPAl*	0.000	0.002	0.000	0.000	0.000	0.000
MS-GARCH-GED	*SPAc*	0.000	0.002	0.000	0.000	0.000	0.000	MS-GARCH-GED	*SPAc*	0.000	0.002	0.000	0.000	0.000	0.000
	RC	0.252	0.442	0.020	0.059	0.006	0.079		RC	0.250	0.453	0.020	0.048	0.011	0.076

Table 11: Note: This table presents the *p*-values of White's (2000) Reality Check test, and Hansen's (2005) Superior Predictive Ability test. The *SPAl* and *SPAc* are the lower and consistent *p*-values from Hansen (2005), respectively. RC is the *p*-value from White's (2000) Reality Check test. Each row contains the benchmark model. The null hypothesis is that none of the alternative models outperform the benchmark. The *p*-values are calculated using 3000 bootstrap replications with a block length of 2.

both studies use an estimation methodology that does not allow for a straightforward calculation of multi-step forecasts. Hence, they only compute one-step-ahead forecasts. Fong and See (2002) use three loss functions (MSE, MAE, which correspond to MSE_2 and MAD_2 in our paper, together with R^2) to evaluate the out-of-sample performance of a MS-GARCH-t and a GARCH-t model in forecasting one-day-ahead volatility. They find that the MS-GARCH-t yields a lower loss when the MSE_2 or MAD_2 are used, however, the ranking is reversed when the R^2 is used. Thus, it is not clear that the switching model performs unanimously better than the non-switching model for a short forecast horizon. In contrast, we evaluate volatility in spot oil prices at the 1-day horizon, where the EGARCH-GED is ranked above the switching models for five out of six loss functions. Yet, the GARCH-t and the MS-GARCH-t are closely tied: the MSE_2 ranks the GARCH-t higher but the MS-GARCH-t is preferred if we use the MAD_2. In other words, had we restricted ourselves to the models and loss functions used by Fong and See (2002), we would have reached similar conclusions. However, our consideration of a larger set of models and loss functions leads us to conclude that an EGARCH-GED performs substantially better than the alternative models.

Nomikos and Pouliasis (2011), on the other hand, consider a wider range of models and forecast evaluation methods than Fong and See (2002) but do not estimate EGARCH models. They instead focus on GARCH, MS-GARCH, and Mix-GARCH and also compute the one-step-ahead forecasts. Overall, they find evidence that the Mix-GARCH-X model yields smaller forecast errors and more accurate forecasts for NYMEX WTI futures. This result is also consistent with our finding that at the 1-day horizon MS-GARCH models are less favorable.

How Stable is the Forecasting Accuracy of the Preferred Models?

One concern with using a single model to forecast over a long time period is that the predictive accuracy might depend on the out-of-sample period used for forecast evaluation.

In particular, a model might be chosen for its highest predictive accuracy when evaluating the loss functions over the whole out-of-sample period, yet one of the competing models might exhibit a lower Mean Squared Predictive Error ($MSPE$) at a particular point (or points) in time during the evaluation period. As we have already mentioned, Tables 4 and 5 indicate that for the evaluation period of the year 2012, the EGARCH-GED and the EGARCH-t exhibit lower $MSPE$ –as measured by the MSE_1 in (11)– for the 1- and 5-day forecast horizons respectively, whereas the MS-GARCH-t results in smaller $MSPE$ for the longer 22- and 66-day horizons. To investigate the stability of the forecast accuracy, we compute the $MSPE$ over 185 rolling sub-samples in the evaluation period, where the first sub-sample consists of the first 66 forecasts (three months) in the evaluation period, the second sub-sample is created by dropping the first forecast and adding the 67th forecast at the end, and so on. In brief, these $MSPE$s are now computed as the average MSE_1 over a rolling window of size $n = 66$. Figure 4 plots the ratio of the $MSPE$ for three out of the four models relative to the "best model" at each of the four horizons, where the best model is selected based on the results reported in Tables 4 and 5, i.e., for the whole evaluation period. Note that, because the last window used to compute the $MSPE$ spans the period between September 26, 2012 and December 30, 2012, the last $MSPE$ ratio is reported at September 25, 2012.
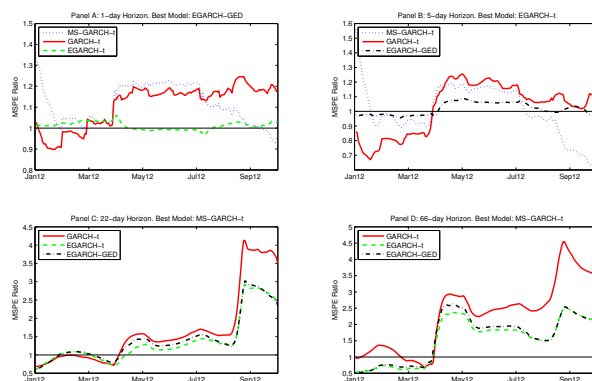

Figure 4: Rolling Window MSPE Ratio Relative to Best Models.

Panel A in Figure 4 illustrates that at the 1-day horizon the EGARCH-GED almost always has higher predictive accuracy than the GARCH-t as evidenced by the $MSPE$ ratio exceeding 1 over almost all of the evaluation period. In contrast, the predictive accuracy of the EGARCH-t and the EGARCH-GED is very similar. Consistent with being ranked lower in Tables 4 and 5, the MS-GARCH-t has lower predictive accuracy than EGARCH-GED for most of the evaluation sample; the only exception being the days in September 2012. Regarding the 5-day horizon (Panel B of Figure 4), the conclusions we draw from the $MSPE$ ratios are very similar to those for the 1-day horizon. Relative to the EGARCH-t, the forecast accuracy of the GARCH-t is considerably worse with the exception of the first quarter of 2012 where the ratio fluctuates around 0.8. That of the EGARCH-GED is comparable, and the accuracy of the MS-GARCH-t is worse during the first month but it is more accurate from July 2012 onwards. As for the longer 1-month and 3-month horizons, the MS-GARCH-t –which exhibits the lowest MSE_1 in Tables 4 and 5 for the out-of-sample period under consideration– has been more accurate than any of the three closest competitors (Panels C and D of Figure 4) during the last two quarters of the evaluation period, especially during the last two quarters of the evaluation period.

We conclude that there are clear gains from using the MS-GARCH-t model for forecasting crude oil return volatility at longer horizons. Whereas these gains are not evident for the 1- and 5-day horizons over the one-year evaluation period (see Table 4), some gains become clear when we plot the ratio of the rolling window $MSPE$s of a sub-period of three months, especially towards the end of the evaluation period.

CONCLUSION

This paper offered an extensive empirical investigation of the relative forecasting performance of different models for the volatility of daily spot oil price returns. Our results suggest four key insights for practitioners interested in crude oil price volatility. First, given the extremely high kurtosis present in the data, models where the innovations are

assumed to follow a Student's t or a GED distribution are favored over those where a normal distribution is presumed. Second, for the one day horizon, nonlinear GARCH models, e.g., the EGARCH-GED and EGARCH-t, are often ranked higher in terms of loss functions and tend to yield more accurate forecasts than other GARCH or MS-GARCH models. Third, as the length of the forecast horizon increases, the MS-GARCH-t model outperforms non-switching GARCH models and other regime switching specifications. Lastly, when we analyzed the stability of the forecasting accuracy over different evaluation periods, we found clear gains from using the MS-GARCH-t model at the longer 1- and 3-months horizons as well as higher predictive accuracy for the 1-day and 5-day horizons towards the end of the evaluation period. All in all, our analysis suggested that the MS-GARCH-t model yields more accurate long-term forecasts of spot WTI return volatility.

Two caveats are needed here. First, as it is well known in the literature, EGARCH models deliver an unbiased forecast for the logarithm of the conditional variance, but the forecast of the conditional variance itself would be biased following Jensen's Inequality (e.g., Anderson et al. 2006, among others). For practitioners who prefer unbiased forecasts, caution must be taken when using EGARCH models. Second, long horizon volatility forecasts that might be of interest to oil companies, such as the 1- and 3-month horizons, may be computed in three different ways. For instance, if a researcher was interested in obtaining a one-month-ahead forecast, she could compute a "direct" forecast by first estimating the horizon-specific (e.g., monthly) GARCH model of volatility and then using the estimates to directly predict the volatility over the next month. Alternatively, as we do here, she could compute an "iterated" forecast where a daily volatility forecasting model is first estimated and the monthly forecast is then computed by iterating over the daily forecasts for the 22 working days in the month. In this paper we use the "iterated" forecast to evaluate the relative out-of-sample performance of different models in the context

of multi-period volatility forecast. Ghysels, Rubia, and Valkanov (2009) find that iterated forecasts of stock market return volatility typically outperform the direct forecasts. Thus we opt for this forecasting scheme. Nevertheless, evaluating the relative performance of these two alternative methods and comparing it to the more recent mixed-data sampling (MIDAS) approach proposed by Ghysels, Santa-Clara, and Valkanov (2005, 2006) is the aim of our future research.

CHAPTER 2: A DURATION ANALYSIS OF NORTH SLOPE OIL WELL DRILLING

INTRODUCTION

Firms face many different types of investment decisions. When the investment is irreversible and the firms are facing uncertain economic conditions, firms must decide the optimal timing to maximize the profits from the investment. In the presence of changing uncertainty, the timing of the irreversible investment is even more important. For example, an electric company must decide when to build a dam for hydroelectric power without knowing what the future demand for electricity will be. Oil firms purchase offshore oil leases without knowing the full extent of the petroleum reserves. In either case, the investment costs cannot be fully recovered should the firm change its plans, thus the costs become sunk.

Real options theory began with Marschak (1949) and Arrow (1968) and has since been advanced by Bernanke (1983), Pindyck (1991) and Dixit and Pindyck (1994). Real options theory describes how firms should time irreversible investments. Irreversible investment is considered an option so that a firm can choose to invest now, or delay investment to observe the evolution of the investment payoff over time. Real options models solve for a trigger price for new investment, P^*. When the price that results from the new investment is larger than the trigger price, a firm will choose to make an irreversible investment. For instance, oil firms determine the price of oil which, given the future expected production of a well, will provide a level of profits that justify undertaking the expense of drilling that well. If the price of oil is lower than the trigger price, the firm delays exercising the option to drill. Real options theory predicts that uncertainty surrounding the price causes firms to delay irreversible investment. In simple real options models when investment is completely irreversible, future asset price is the only source of uncertainty. An important feature of real options theory is that delaying the option has value since both positive and

negative returns are possible.

Because I lack detailed drilling cost data and the ability to estimate profits and a specific trigger price, P^*, my empirical approach is to identify the implication of a higher P^* by estimating the hazard rate of drilling. A decrease in the hazard rate would signify a delay in drilling, or an increase in the time between investments and imply a higher P^*. I collect data from the Alaska Oil and Gas Conservation Commission (AOGCC) which contains the dates and other characteristics of oil wells drilled on the North Slope of Alaska from July 2003 to December 2014. Using a discrete proportional hazards model with a Weibull distribution, I estimate the hazard rate of drilling and the effect of uncertainty on the timing of the investment.

Consider an oil firm that must decide when to drill an oil well in the presence of uncertainty in oil prices. There are three main reasons why an oil well is an excellent example of an irreversible investment. First, on the North Slope of Alaska, there is a significant cost involved in drilling an oil well. Once a well is drilled, the materials and labor used in drilling an oil well cannot be recovered and reused for an alternative project. The cost incurred drilling an oil well is a sunk cost and thus irreversible. Second, drilling of oil wells occurs in discrete bursts, followed by periods of inactivity. The discrete nature of investments on the North Slope allows for examination of the timing of the drilling and to observe how the timing changes in the presence of uncertainty. Third, oil companies on the North Slope are price takers in a highly competitive industry. Oil is priced on the world market, and thus no single company has the ability to impact the world price of oil.

Recent papers that investigate the impact of uncertainty on investment include Bulan, Mayer, and Somerville (2009) who use a GARCH (1,1) specification to model the volatility of monthly neighborhood returns and the impact on condominium investment in Vancouver from 1979 to 1998. The authors find that an increase in the volatility of

one standard deviation resulted in a decrease in investment of 13 percent. Dunne and Mu (2010) study refinery investments using a hazard model and find that when uncertainty increases, the probability that a refinery adjusts its capacity decreases. Moel and Tufano (2002) investigate gold mine closings using real options theory and find both the price and volatility of gold influence the closing of mines. Hurn and Wright (1994) find that while oil prices and level of reserves shorten the appraisal duration of North Sea oil fields, oil price variability does not. Kellogg (2014) investigates infill oil drilling in Texas from 1993 to 2003 using monthly data on oil wells drilled in sole-operated oil fields. He uses implied volatility constructed from NYMEX 18-month oil price futures to estimate a dynamic model of firms' response to oil price volatility. Kellogg (2014) finds that firms reduce drilling when oil price uncertainty rises and the magnitude of the reduction is consistent with predictions from real options theory.

I analyze the effect of oil price volatility on the hazard rate of drilling development oil wells in Alaska. Boyce and Nøstbakken (2011) develop a model of exploration and development for crude oil and natural gas fields for the entire United States, including Alaska. They find that exploration and development wells have been declining and increasing respectively, over time. Whereas they use annual aggregate data for total wells drilled and did not include any measure of price uncertainty, I use individual well drilling data and include several different oil price volatility measures. Leighty and Lin (2012) study changes in Alaska's North Slope oil production in response to variations in tax policy, investigating several different combinations of tax rates and tax credits. Estimating field specific cost functions and field specific production functions, they find that the tax rate alone does not alter the optimum oil production path, but the tax structure, i.e., high tax rates on gross well-head value coupled with a low amount of tax credits, can impact the optimum path. Leighty and Lin (2012) include past production of each field as well as known oil reserves, but do not consider the effect of uncertainty in oil prices on oil

production or well drilling.

Using a duration analysis, I investigate the effect of oil price uncertainty on onshore oil well drilling on the North Slope of Alaska. Data on individual oil wells on the North Slope was obtained from the Alaska Oil and Gas Conservation Commission (AOGCC) from July 2003 to December 2014. As with Kellogg (2014), and Leighty and Lin (2012), I take advantage of the competitive nature of the oil industry, with oil prices set by the world market, and firms having little ability to impact oil prices. I avoid the complication of using aggregate data since I have data on the individual investment of drilling oil wells.

I find that the hazard rate of drilling an oil well on the North Slope is negatively related to uncertainty, both in aggregate and at the field level. The effects vary with the choice of the volatility measure. If using a GARCH (1,1), and EGARCH (1,1) of a GJR-GARCH (1,1) forecast, the overall effect of uncertainty on the hazard rate of drilling on the North Slope is negative and about 0.8%. When using realized volatility, the probability of drilling a new well declines by about 0.16% for a one percent increase in volatility.

OIL DRILLING IN ALASKA

The North Slope of Alaska is composed of seven different oil fields: Badami, Colville River, Kuparuk River, Milne Point, Nikaitchuq, Oooguruk, and Prudhoe Bay. Table 12 presents the fields and the number of wells drilled during the sample period. Between July 2003 and December 2014, 562 wells were drilled in Prudhoe Bay, the most of all fields. Kuparuk River is next with 381 wells drilled. This study focuses on the most active fields on the North Slope. Thus, Badami and Oooguruk are excluded from the duration analysis since each field had a single well drilled during the sample period.

Oil is a natural resource found in underground reservoirs created by geologic formations. Accessing a reservoir in order to deliver the oil to the market requires a firm to drill a hole into the pocket of oil beneath the surface. As the firm drills into the ground,

North Slope Field Information

Field	Start Date	Wells Drilled	Side Tracks
Colville River	Nov-00	66	17
Badami	Aug-98	1	0
Kuparuk River	Dec-81	344	283
Milne Point	Nov-85	61	38
Nikaitchuq	Jan-11	22	8
Oooguruk	Mar-03	1	0
Prudhoe Bay	Apr-69	562	498

Table 12: Wells drilled is the number of wells drilled in each field during the sample period: July 1, 2003 to December 31, 2014. Side Tracks is the number of side tracks drilled in the sample period.

steel pipe is used to line the well bore, and cemented in place for stability. Once accessed, the oil is pumped to the surface and transported to the market. Productive oil wells can continue to produce oil for many years.

Since the labor, steel pipe used for the casing, and the costs for the drilling rig rental are not recoverable, the investment into the drilling of a well can be modeled as an irreversible investment. Once a well is drilled it is permanent. Thus, before a firm decides to make the investment to drill a well, it must also consider the benefits that result from a productive well (Kellogg, 2014). The firm does not know with certainty the price of oil once production begins, therefore it must form an expectation on the price of oil in advance of the decision to drill.

METHODS

Duration Model

The main goal of this chapter is to examine the implication of uncertainty on the hazard rate of drilling an oil well. Irreversible investment theory implies that the timing of investments is affected by uncertainty; higher uncertainty leads firms to delay an irreversible investment. Bigsten et al. (2005) find positive correlation in investment and the prediction of negative duration dependence in the hazard function in models with irre-

versibility. A key difference between models with irreversibility and convex adjustment cost models, is that convex adjustment cost models assume that firms smooth investments across time whereas models with irreversibility have periods of investment inactivity intermixed with discrete bursts of investment (Dunne and Mu, 2010). Because the North Slope features periods of investment inactivity and drilling an oil well is an exit from the inactivity, a discrete proportional hazards model can be used to estimate the effects of uncertainty on the timing of the exit.

Oil wells on the North Slope are drilled from structures known as drilling pads, which are described in the next section. Most of the pads in the sample are used multiple times: there are 103 pads and 1055 development wells drilled during the sample period. The duration in months between investment episodes is the time in months between two wells being drilled from the same drilling pad. The mean duration for the sample period is 9.47 months and the median duration is 1.96 months. After each investment episode the duration clock is reset to zero.

I begin by defining T to be the length of inactivity of a drilling pad on the North Slope. The cumulative probability distribution of T is specified by:

$$F(t) = Pr(T \leq t)$$

Then, the probability that a drilling pad stays inactive longer than T is given by the survivor function:

$$S(t) = 1 - F(t) = Pr(T > t)$$

The hazard function gives the conditional probability that a drilling pad exits from a period of inactivity in the interval Δt after it is inactive until time t (Kiefer 1988). The

hazard function can be written as:

$$h(t) = \lim_{\Delta t \to 0} \frac{Pr(t \leq T < t + \Delta t | T \geq t)}{\Delta t}$$

The general functional form of the parametric proportional hazards model is given by:

$$h(t|x_j) = h_0(t)exp(x_j\beta_x) \tag{19}$$

where $h_0(t)$ is the baseline hazard function, x_j is a vector of explanatory variables, and β_x are the corresponding coefficients to be estimated from the data. Although there are different ways to specify $h_0(t)$, I assume a Weibull distribution following Dunne and Mu (2010) and Hurn and Wright (1994). The baseline hazard with a Weibull distribution becomes:

$$h_0(t) = pt^{p-1}exp(\beta_0) \tag{20}$$

where p is an estimated ancillary shape parameter and $exp(\beta_0)$ is the scale parameter. The Weibull distribution accommodates both monotonically increasing and decreasing shapes of the hazard function, which is determined by the estimated shape parameter, p. If $p > 1$, the hazard increases with t; if $p = 1$, the hazard is constant and the model reduces to an exponential distribution; if $p < 1$, the hazard decreases with t. The hazard function gives a definition of duration dependence. If the probability that investment inactivity ends increases as the length of inactivity increases, then positive duration dependence is present. Negative duration dependence is then defined as: the probability of investment inactivity ending decreases as the length of inactivity increases. Positive and negative dependence is also referred to as increasing and decreasing hazard, respectively (Kiefer, 1998).

Given a set of covariates, x_j, and combining (19) and (20), the model becomes:

$$h(t|x_j) = h_0(t)exp(x_j\beta_x) = pt^{p-1}exp(\beta_0 + x_j\beta_x) \tag{21}$$

Equation (21) is estimated for all the North Slope fields pooled together using the explanatory variables described in the next section. In addition, (21) is estimated for each of the five most active fields during the sample period.

DATA

Monthly West Texas Intermediate (WTI) crude oil spot prices were obtained from the U.S. Energy Information Administration. Monthly real oil prices in 1982 dollars are obtained by deflating the nominal oil price with the producer price index obtained from the St. Louis FRED. The sample period ranges from July 2003 until December 2014. The 5 fields included have been the most active since 2003. Over this time period, the monthly average real price of a barrel of crude oil was \$41.26 and the standard deviation was \$9.40. A maximum price \$66.77 was observed in June 2008, possibly due to geopolitical tensions in the Middle East. Descriptive statistics are listed in Table 13.

Descriptive Statistics

	Mean	St. dev	Min	Max
WTI	41.26	9.40	20.44	66.77
TVD	7142.54	1918.2	351	13662
RigCount	7.94	2.22	3	17
TundraDays	138.58	13.71	112	161
SideTrack	0.80	0.40	0	1

Table 13: WTI denotes the monthly price of the West Texas Intermediate spot price deflated to 1982 dollars using producers price index; TVD is the total vertical depth of the wells drilled from July 1, 2003 to December 31, 2014; $RigCount$ is obtained from Baker Hughes Weekly Rig Count for North America; $TundraDays$ represents the number of days the tundra is open to travel, obtained from Alaska DNR. $SideTrack$ is a dummy variable equal to 1 if the well drilled is a new well or a side track well, zero otherwise.

GARCH Models

Real options models assume that firms will use a forward-looking measure of volatility in deciding when to drill a well. I compare the results when considering GARCH (1,1),

EGARCH (1,1), and GJR-GARCH (1,1) volatility forecasts as the volatility measure. In chapter 1, daily oil price returns exhibited ARCH effects, however, in this section monthly oil prices are used. Therefore, testing for ARCH effects is repeated. Monthly returns are regressed on a constant and residuals are tested for autocorrelation and ARCH effects. The Breusch-Godfrey test rejects the null of no serial autocorrelation and the LM test for ARCH effects strongly rejects the null of no ARCH effects in all lag orders from 1 to 20. The $p-$values for both tests are all 0. Therefore, the mean equation is re-specified to include one AR term to eliminate serial correlation. It is found that an AR(1) specification is sufficient to eliminate serial correlation, and also minimizes AIC for all lags 1 to 20. Thus, the conditional mean equation from (1) in chapter 1 is now estimated: $r_t = \mu + r_{t-1} + \varepsilon_t$.

Figure 5 plots the returns of the monthly WTI spot prices and the squared deviations from January 1986 to December 2014. Similar to Figure 1, which plots daily returns, large variations are observed during the crude oil price crises in 1986 and 1988, Middle East conflicts in late 1990 and early 1991, the financial crisis in 2008, and the oil price collapse of late 2014. Figure 5 suggests monthly crude oil returns are characterized by periods of low volatility followed by high volatility throughout the sample period.

I forecast oil price volatility using the traditional GARCH model in (1), and also include EGARCH, (7), and GJR-GARCH models, (6), discussed in Chapter 1. One possible shortcoming of the standard GARCH model is the assumption that shocks have symmetrical effects on the conditional variance. The benefits of including the nonlinear EGARCH and GJR-GARCH models are the ability to capture leverage effects, volatility clustering, and fat tails. In addition, generating forecasts using these models is relatively straightforward and have been shown to perform well with short out-of-sample oil price volatility forecasts (Mohammadi and Su 2010, and Hou and Suardi 2012). For each model, I estimate three different error distributions: Normal, Student's t, and Generalized Error
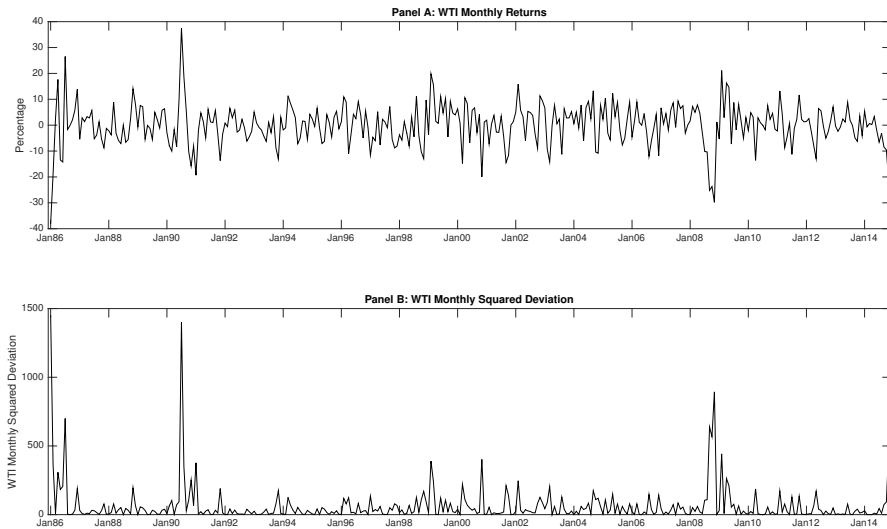
Figure 5: Monthly WTI Crude Oil Returns and Squared Deviations. The sample period extends from January 1986 through December 2014.

Distribution.

To construct the GARCH volatility forecasts for the sample period, July 2003 to December 2014, I start by estimating the GARCH models for a sample of January 1986 to June 2003 using 209 observations. I then forecast the one-step ahead volatility for July 2003. To forecast the volatility for August 2003, I drop one observation at the beginning of the sample and add one observation at the end. The process continues for each of the remaining months in the sample period, forecasting one month ahead volatilities using a rolling window of 209 observations of real oil prices.

Realized Volatility

As a comparison to the various GARCH model forecasts, I also include realized volatility calculated from 5-minute prices of 1-month West Texas Intermediate (WTI) futures contracts for NYMEX Light Sweet Crude Oil, symbol CL, from Tickdata.com. Following the same procedure described in chapter 1, I construct daily realized volatility by taking the sum of the intraday 5-minute returns during trading hours, (9:30am to 4:00pm EST) and then adding the square of the previous overnight return. The sample period

Realized Volatility Descriptive Statistics

	Mean	St. dev	Skewness	Kurtosis
$RV^{1/2}$	0.019	0.011	3.04	22.96
$Log(RV^{1/2})$	-4.08	0.47	0.24	3.84

Table 14: RV denotes realized volatility computed from the 5-minute returns of oil futures. $RV^{1/2}$ and the natural logarithm of $RV^{1/2}$ series are from July 1, 2003 to December 31, 2014 for 2895 observations.
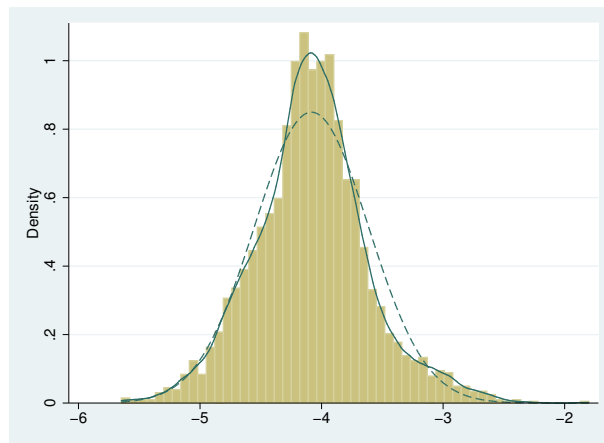

Figure 6: $\ln(RV^{1/2})$ distributions. The sample period extends from July 1, 2003 through December 31, 2014. The solid line is the kernel density. The dotted line is a normal density scaled to have the same mean and standard deviation of the data.

ranges from July 1, 2003 to December 31, 2014 for a total of 2895 observations. Summary statistics for daily $RV_t^{1/2}$ and the logarithm of daily $RV_t^{1/2}$ are listed in Table 14. The $RV_t^{1/2}$ series is right-skewed and leptokurtic. Similar to the summary statistics presented in Table 1, the logarithm of $RV_t^{1/2}$ is closer to a normal distribution and comparing its kernel density estimates with the normal distribution in Figure 6 is similar to what is seen in Figure 2. Monthly RV_t is then constructed by summing the daily realized volatility over the month with $m = 21$:

$$\widehat{RV}_{T,T+m} = \sum_{j=1}^{m} \widehat{RV}_{T+j}.$$

Remaining Explanatory Variables

Unlike other states such as Texas, where landowners own the rights to minerals beneath their land, the state of Alaska owns the rights to the oil and gas contained in subterranean

reservoirs. Thus, firms interested in development of an oil reservoir on the North Slope purchase leases from the state during periodic lease sales. Each lease represents an option to drill for oil, and firms may or may not exercise the option. In the sample period, many firms drill multiple producing wells on a single lease. When multiple firms own leases above the same oil field, the common pool problem can arise. To prevent this, Alaska statute allows the firms to form a unit (Alaska Stat.§31.05.110). The unit agreement prevents the common pool problem by requiring all the firms holding leases above the oil field to agree to a development plan and choose a single firm to operate the field before developing the field. All the fields in this study are part of a unit (AOGCC website). Number of leases are included as an indication of a firm's level of interest in the oil field.

Alaska imposes seasonal limits on North Slope during the summer months, which introduces two unique aspects for firms operating on the North Slope. The first is restricted winter travel. During the winter months, over the tundra travel starts when the DNR determines that conditions are suitable to open the tundra to general off-road travel. Opening and closing dates for over the tundra travel from 2003 through 2014 were obtained from the Alaska DNR. The longest travel season was 161 days in 2004-2005, and the shortest season of 120 days occurred in 2008-2009. Table 13 presents the summary statistics. Secondly, firms are limited in the places where an oil well can be drilled. To access the subterranean oil, most often a company must drill from an existing drilling pad. A drilling pad is a gravel platform built on the tundra and allows for the operation of drilling rigs while protecting the tundra from damage. The sample contains 103 drilling pads and most pads are used to drill multiple wells during the sample period. Drilling from existing drilling pads means that in order to access the reservoir, well bores often have to be several thousand feet long to reach the oil in parts of the reservoir not directly underneath the drilling pad. The total vertical depth of the wells drilled in the sample is included as an indication of the total cost of drilling a well, and summary statistics are

presented in Table 13.

The well bore paths have become more complex as drilling technology has improved over the past 30 years, and relatively sharp changes in hole angle and direction are now possible (See Figure 7). Coiled-tubing drilling is used to drill side tracks, which are smaller diameter, relatively flexible pipe that coils on a very large spool rather than standard, thick-walled, straight drill pipe. This enables operating companies to reach smaller oil accumulations within major oil fields. Coiled tubing has become settled technology on the North Slope (Gantt et al.,1998). The number of side tracks drilled in each field during the sample period are included in Table 12.
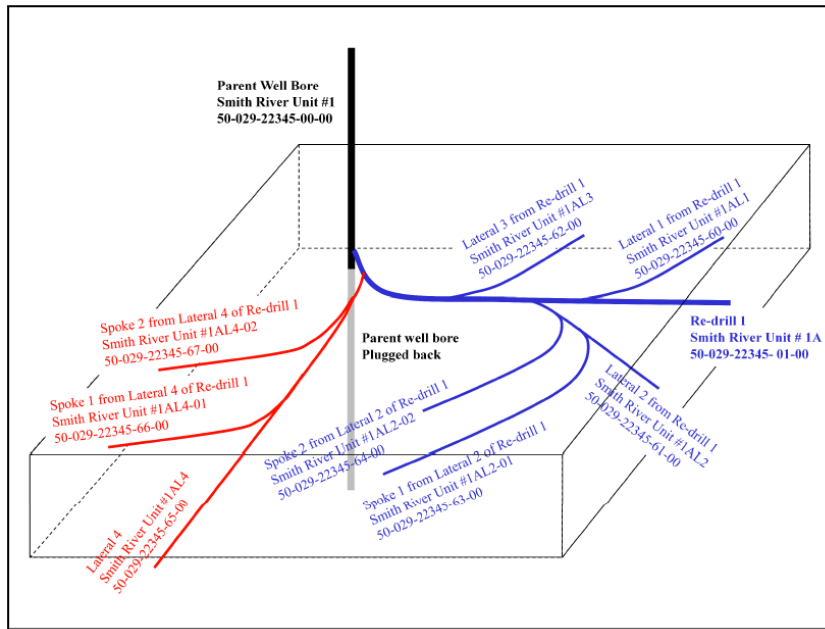
Figure 7: Illustration of complex well bore paths possible using coiled tubing drilling. Source: AOGCC

Data on the number of drilling rigs available in Alaska were obtained from the Baker Hughes North American rig count. Baker Hughes releases the weekly rig count for North America on the last working day of the week. The count contains onshore rigs that are actively drilling. Table 13 presents the summary statistics. The average number of rigs actively drilling during the sample period is 7.95, and the maximum number of rigs is 17,

occurring in February 2014. There are a limited number of drilling rigs, and there were recent instances where demand exceeded supply (personal communication, manager with Nabor's Drilling Company, April 2012)

RESULTS

I estimate the hazard model in (21) by maximum likelihood.[26] The baseline hazard, $h_0(t)$ reflects the probability of a well being drilled only as a function of time. The explanatory variables multiplicatively affect the probability of drilling a well by the factor e^β. In the hazard model, the null hypothesis of $\beta = 0$ corresponds to a coefficient equal to 1. In the results that follow, the coefficient on a variable x that is estimated is the proportional effect on the hazard rate of a unit change in x. Then a one unit change in x leads to a $100 * e^{\beta_x - 1}$ percent change in the hazard rate. If the impact on the baseline hazard is positive, the estimated coefficient is greater than one, that is, a higher probability of drilling an oil well. The reverse is also true - a hazard ratio less than one reduces the probability of drilling. Robust standard errors are estimated using the Huber/White estimator clustered on each individual drilling pad in the sample to allow for correlation across time in the hazard rate of individual fields.

One complication is that I do not observe the date the decision to drill is made. According to a petroleum geologist with the AOGCC, an application for a permit to drill is usually approved in less than ten days. The average time for drilling a well in the sample period is 22 days, and most wells in the sample period are completed within 90 days. Thus, to accommodate the length of time it takes to decide when to drill, RV and $RealOilPrice$ are lagged three months.

Each model is estimated using GARCH (1,1), EGARCH (1,1), and GJR-GARCH (1,1) forecasts, with three error distributions: Normal, Student's t, and GED; the results are presented in Tables 15, 16, and 17. The estimates for the three duration models

---

[26]The streg command with STATA was used to perform the duration analysis.

		Duration Models: GARCH Forecasts All Fields									
	Model I	Model II	Model III		Model I	Model II	Model III		Model I	Model II	Model III
$GARCH$	0.9908***	0.9911***	0.9908***	$GARCH-t$	0.9904***	0.9906***	0.9904***	$GARCH-GED$	0.9904***	0.9907***	0.9904***
	(0.0017)	(0.0016)	(0.0016)		(0.0017)	(0.0016)	(0.0016)		(0.0016)	(0.0016)	(0.0016)
$RealOilPrice$	0.9232***	0.9172***	0.9148***	$RealOilPrice$	0.9223***	0.9159***	0.9134***	$RealOilPrice$	0.9215***	0.9154***	0.9129***
	(0.0089)	(0.0093)	(0.0095)		(0.0090)	(0.0094)	(0.0097)		(0.0088)	(0.0092)	(0.0095)
$Tundra$		0.6949***	0.7092***	$Tundra$		0.6967***	0.7109***	$Tundra$		0.7010***	0.7151***
		(0.0866)	(0.0882)			(0.0867)	(0.0883)			(0.0871)	(0.0888)
$NumLeases$		0.9986	0.9975	$NumLeases$		0.9986	0.9975	$NumLeases$		0.9986	0.9975
		(0.0018)	(0.0019)			(0.0018)	(0.0019)			(0.0018)	(0.0019)
TVD		0.8886**	0.8445***	TVD		0.8880**	0.8436***	TVD		0.8880**	0.8434***
		(0.0541)	(0.0584)			(0.0540)	(0.0586)			(0.0538)	(0.0582)
$RigCount$		0.9549	0.9632	$RigCount$		0.9527	0.9609	$RigCount$		0.9532	0.9616
		(0.0295)	(0.0299)			(0.0296)	(0.0301)			(0.0294)	(0.0299)
$SideTracks$			1.6303**	$SideTracks$			1.6313**	$SideTracks$			1.6382**
			(0.3132)				(0.3147)				(0.3155)
Constant	0.4779***	2.6042	3.0850	Constant	0.5161***	2.9314	3.4872	Constant	0.5040**	2.8060	3.3420
	(0.1897)	(2.2053)	(2.7692)		(0.0214)	(2.5245)	(3.2000)		(0.1972)	(2.3716)	(2.9994)
p	1.52***	1.56***	1.56***	p	1.51***	1.56***	1.56***	p	1.53***	1.57***	1.57***
	(0.0678)	(0.0654)	(0.0647)		(0.0667)	(0.0643)	(0.0637)		(0.0679)	(0.0656)	(0.0649)
LL	848.62	891.84	907.55	LL	849.88	893.72	909.44	LL	853.06	896.13	912.17

Table 15: Results for the duration models when pooling all fields and GARCH(1,1) forecasts with Normal, Student's t, and GED errors are the volatility measures. Hazard ratios are reported; ***, **, and * denote hazard ratios that are different from one at the 1%, 5%, and 10%, respectively. Robust standard errors are in parenthesis. TVD: total vertical depth of the well in '000's of feet.

		Duration Models: EGARCH Forecasts All Fields									
	Model I	Model II	Model III		Model I	Model II	Model III		Model I	Model II	Model III
$EGARCH$	0.9911***	0.9910***	0.9913***	$EGARCH-t$	0.9923***	0.9915***	0.9916***	$EGARCH-GED$	0.9926***	0.9917***	0.9918***
	(0.0022)	(0.0022)	(0.0022)		(0.0014)	(0.0014)	(0.0014)		(0.0014)	(0.0014)	(0.0014)
$RealOilPrice$	0.9495***	0.9412***	0.9411***	$RealOilPrice$	0.9428***	0.9311***	0.9305***	$RealOilPrice$	0.9428***	0.9308***	0.9304***
	(0.0079)	(0.0081)	(0.0082)		(0.0084)	(0.0084)	(0.0086)		(0.0084)	(0.0083)	(0.0085)
$Tundra$		0.6479***	0.6629***	$Tundra$		0.6185***	0.6314***	$Tundra$		0.6155***	0.6282***
		(0.0825)	(0.0855)			(0.0746)	(0.0768)			(0.0739)	(0.0762)
$NumLeases$		0.9986	0.9977	$NumLeases$		0.9992	0.9982	$NumLeases$		0.9900***	0.9981
		(0.0018)	(0.0019)			(0.0018)	(0.0019)			(0.0018)	(0.0019)
TVD		0.8807**	0.8440***	TVD		0.8816**	0.8424***	TVD		0.8803**	0.8425***
		(0.0555)	(0.0601)			(0.0547)	(0.0596)			(0.0547)	(0.0594)
$RigCount$		0.9800	0.9864	$RigCount$		0.9728	0.9793	$RigCount$		0.9683	0.9748
		(0.0304)	(0.0312)			(0.0310)	(0.0319)			(0.0306)	(0.0314)
$SideTracks$			1.4832*	$SideTracks$			1.5185*	$SideTracks$			1.4987*
			(0.2847)				(0.2943)				(0.2886)
Constant	0.1819***	0.9378	1.0089	Constant	0.2141***	1.2731	1.4213	Constant	0.2169***	1.4268	1.5695
	(0.0864)	(0.8470)	(0.9439)		(0.0977)	(1.1551)	(1.3425)		(0.0990)	(1.2849)	(1.4677)
p	1.46***	1.51***	1.51***	p	1.49***	1.55***	1.55***	p	1.48***	1.55***	1.54***
	(0.0694)	(0.0632)	(0.0641)		(0.0690)	(0.0627)	(0.0641)		(0.0684)	(0.0617)	(0.0408)
LL	822.32	871.11	881.02	LL	835.41	890.43	901.59	LL	835.10	892.03	902.53

Table 16: Results for the duration models when pooling all fields and EGARCH(1,1) forecasts with Normal, Student's t, and GED errors are the volatility measures. Hazard ratios are reported; ***, **, and * denote hazard ratios that are different from one at the 1%, 5%, and 10%, respectively. Robust standard errors are in parenthesis. TVD: total vertical depth of the well in '000's of feet.

using RV as the volatility measure are presented in Table 18. The first column contains the estimates for the Model I, only including the volatility measure and real oil prices, $RealOilPrice$, as explanatory variables. To capture other specific characteristics that may impact the decision to drill a well, the second column presents the results of the Model II adding the explanatory variables discussed in the Data section, while the third column, Model III, also includes the dummy variable for side track wells.

The first result to note is that for all the various volatility measures, p is significantly greater than one at the 1% level, indicating that the hazard is increasing with time. In other words, the probability of drilling increases as the time since the last drilling episode

Duration Models: GJR-GARCH Forecasts All Fields

	Model I	Model II	Model III		Model I	Model II	Model III		Model I	Model II	Model III
GJR	0.9907***	0.9909***	0.9907***	*GJR − t*	0.9907***	0.9908***	0.9905***	*GJR − GED*	0.9905***	0.9906***	0.9904***
	(0.0015)	(0.0015)	(0.0015)		(0.0015)	(0.0015)	(0.0015)		(0.0014)	(0.0014)	(0.0014)
RealOilPrice	0.9159***	0.9102***	0.9076***	*RealOilPrice*	0.9177***	0.9114***	0.9088***	*RealOilPrice*	0.9134***	0.9072***	0.9048***
	(0.0098)	(0.0103)	(0.0106)		(0.0099)	(0.0104)	(0.0107)		(0.0101)	(0.0104)	(0.0107)
Tundra		0.7144***	0.7280***	*Tundra*		0.7158***	0.7294***	*Tundra*		0.7182***	0.7308***
		(0.0886)	(0.0902)			(0.0885)	(0.0901)			(0.0886)	(0.0900)
NumLeases		0.9985	0.9975	*NumLeases*		0.9985	0.9974	*NumLeases*		0.9985	0.9975
		(0.0018)	(0.0019)			(0.0018)	(0.0019)			(0.0018)	(0.0019)
TVD		0.8870**	0.8430***	*TVD*		0.8870**	0.8427***	*TVD*		0.8852**	0.8415***
		(0.0533)	(0.0577)			(0.0533)	(0.0579)			(0.0531)	(0.0574)
RigCount		0.9533	0.9617	*RigCount*		0.9504*	0.9586	*RigCount*		0.9522	0.9605
		(0.0292)	(0.0296)			(0.0291)	(0.0296)			(0.0291)	(0.0294)
SideTracks			1.6286**	*SideTracks*			1.6321**	*SideTracks*			1.6255**
			(0.3092)				(0.3111)				(0.3064)
Constant	0.5656**	3.1334	3.7042	Constant	0.5221**	3.0565	3.6286	Constant	0.5987*	3.4683	4.0724
	(0.2172)	(2.5875)	(3.2448)		(0.2019)	(2.5380)	(3.2114)		(0.2273)	(2.8477)	(3.5434)
p	1.56***	1.60***	1.60***	*p*	1.56***	1.60***	1.60***	*p*	1.57***	1.61***	1.62***
	(0.0737)	(0.0719)	(0.0714)		(0.0741)	(0.0726)	(0.0721)		(0.0752)	(0.0736)	(0.0729)
LL	863.28	905.06	920.73	*LL*	863.19	905.69	921.49	*LL*	869.72	912.10	927.71

Table 17: Results for the duration models when pooling all fields and GJR-GARCH(1,1) forecasts with Normal, Student's t, and GED errors are the volatility measures. Hazard ratios are reported; ***, **, and * denote hazard ratios that are different from one at the 1%, 5%, and 10%, respectively. Robust standard errors are in parenthesis. TVD: total vertical depth of the well in '000's of feet.

Duration Model: RV All Fields

	Model I	Model II	Model III
RV	0.9982***	0.9984***	0.9984***
	(0.0005)	(0.0005)	(0.0005)
$RealOilPrice$	0.9475***	0.9422***	0.9404***
	(0.0083)	(0.0088)	(0.0090)
$Tundra$		0.6784***	0.6947***
		(0.0857)	(0.0877)
$NumLeases$		0.9986	0.9975
		(0.0018)	(0.0019)
TVD		0.8949*	0.8514**
		(0.0580)	(0.0621)
$RigCount$		0.9751	0.9839
		(0.0310)	(0.0314)
$SideTracks$			1.6315*
			(0.3331)
Constant	0.1105***	0.4396***	0.5379
	(0.0523)	(0.0394)	(0.5380)
p	1.51***	1.55***	1.55***
	(0.0688)	(0.0612)	(0.0617)
LL	860.88	898.68	913.12

Table 18: Results for the duration model. Hazard ratios are reported; ***, **, and * denote hazard ratios that are different from one at the 1%, 5%, and 10%, respectively. RV and $RealOilPrice$ are lagged 3 months. Robust standard errors are in parenthesis. TVD: total vertical depth of the well in '000's of feet.

increases. For all the models and volatility measures, the coefficients on the volatility measure are all significantly less than one at the 1% level.

The second notable result is the magnitudes of the coefficients for all the GARCH forecasts are close to the coefficients when RV is used. Specifically, when considering GARCH volatility forecasts, coefficients are all around 0.99 for all the different forecast specifications. The coefficients are all significantly less than one at the 1% level and are robust both to the choice of GARCH model and to the choice of error distribution. When using RV as the volatility measure, the coefficients range from 0.9982 in the simplest duration model to 0.9984 when including all of the explanatory variables. In response to a one unit increase in volatility, the hazard rate of drilling is reduced by about 0.8% when using GARCH, and 0.16% when using RV.

The third notable result is that $RealOilPrice$ has a negative relationship with the hazard rate of drilling and is significantly different from one at 1% for all estimated models. There is more variability in the effects of real oil prices when comparing models using various GARCH forecasts and models using RV. For instance, when using GARCH (1,1) with normally distributed errors, (See Table 15), the magnitude of the coefficients on $RealOilPrice$ varies from 0.9232 in Model I to 0.9148 in Model III. If instead, forecasts created with Student's t errors are used as the volatility measure, the magnitudes of the coefficients vary from 0.9223 to 0.9134. Finally, when using GED errors, the coefficients on the volatility measure vary from 0.9215 to 0.9129. Each choice of error distribution displays the same pattern: a smaller impact on the hazard rate of drilling in Model I than Models II and III, with Model III having the largest negative impact.

For EGARCH (1,1) or GJR-GARCH (1,1), the pattern is the same, albeit with slightly different magnitudes for the coefficients. GJR-GARCH (1,1) with GED errors is the forecast model which yields the largest negative effects from real oil prices: about a 9.99% decline in the hazard rate of drilling with a $1 increase in the real oil price. When

considering *RV* as the volatility measure, the coefficient on *RealOilPrice* varies from 0.9475 to 0.9404, corresponding to a decrease in the hazard rate of 5.39% to 6.14% for every dollar increase in real oil prices.

Considering the other variables in Models II and III, the coefficients on the length of time the tundra is open has a significant effect on the hazard rate of drilling, in both cases reducing the probability of drilling. This is expected as the restrictions on over the tundra travel imposed by the state reduce the drilling season each year. On average, the tundra is open for travel for just over one third of the year. The coefficents on total vertical depth indicate that the deeper the well, the lower the hazard rate of drilling a well. The impact of the number of leases is statistically insignificant when pooling all of the fields, although the effect of the number of leases is significant when examining several of the fields individually. Since firms have a choice between drilling a new vertical well or a side track well (See Figure 7), the models are estimated with a dummy variable equal to one if the well drilled is a sidetrack, and zero otherwise. Side tracks are cheaper to drill, and they represent a large percentage of the wells drilled on the North Slope (U.S. Department of Energy, National Energy Technology Laboratory [DOE/NETL], 2005). Table 12 presents the number of side tracks drilled in each field, and Figure 8 shows the yearly count of new vertical wells and side track wells drilled from July 2003 to December 2014. Side tracks are more likely to be drilled because, in most cases, the fields are mature and economic conditions allow for the access of smaller pools of oil that were neglected when the fields were initially developed. Also, according to some estimates, the cost of drilling a side track can be up to 50% of the cost of drilling a new vertical well (DOE/NETL, 2005).

The coefficients on the side track dummy variable across the GARCH forecasts all have a positive impact on the hazard rate of drilling, and are significant. For the three GARCH (1,1) error distributions, the coefficients range from 1.6303 for the Normal distribution to 1.6382 for the GED distribution. When using EGARCH (1,1) forecasts for the volatility
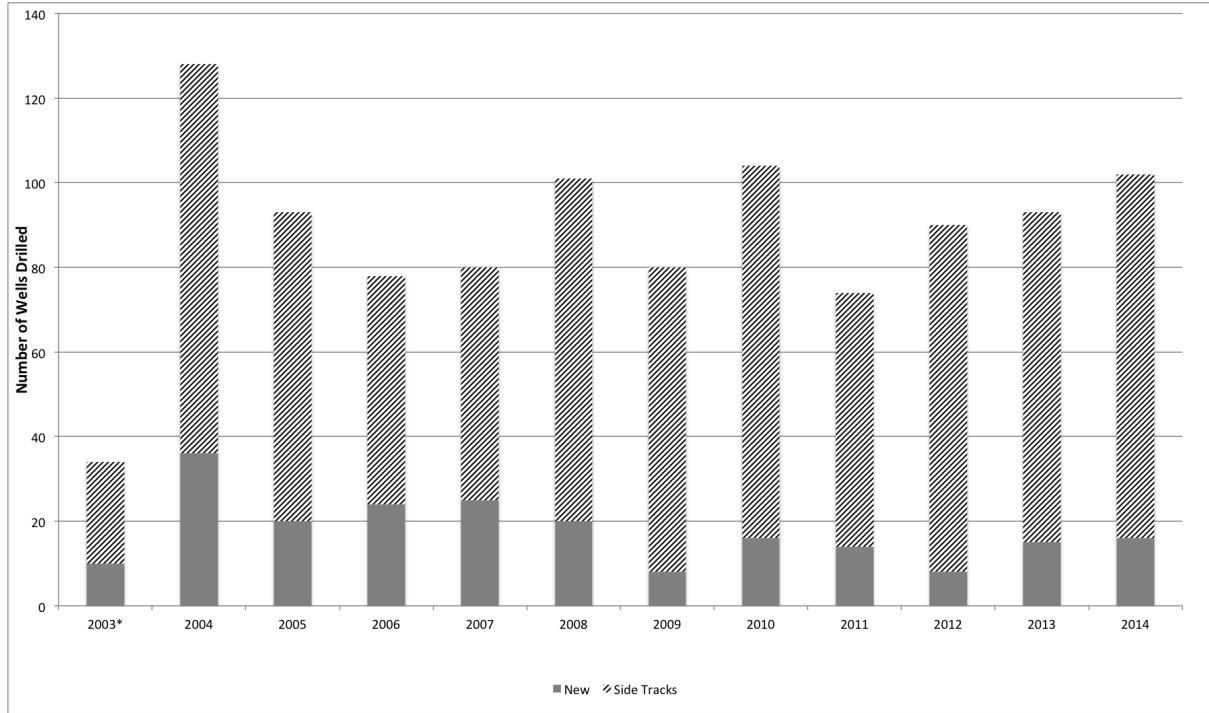
Figure 8: Yearly count of new wells and sidetracks drilled on the North Slope of Alaska. * 2003 starts from July. Source: AOGCC

measure, the t distribution has the largest effect at 1.5185, whereas the Normal has the smallest, 1.4832. For the GJR (1,1) forecasts in Table 17, the Normal distribution has the largest magnitude, 1.6286; the t distribution the smallest, 1.6321. Recall that the coefficients are exponentiated, thus a coefficient equal to one is equivalent to $\beta = 0$. Compared with a coefficient of 1.6315 for RV, the effects of the various GARCH forecasts similar for GARCH and GJR-GARCH, but smaller for EGARCH.

The log-likelihoods of the models estimated using GARCH forecasts have a smaller log-likelihood than those using RV. However, when GJR-GARCH forecasts are used, the log-likelihoods are larger than the models estimated using RV. In addition, the magnitudes of the log-likelihoods for the models estimated using GARCH, GJR-GARCH, and RV volatility measures are similar in magnitude, while EGARCH models are lower for each error distribution; although a direct comparison between GARCH and EGARCH

forecasts are difficult due to potential differences in the magnitude of the forecasts.

To further investigate the effects of volatility on the drilling activity on the North Slope, Model III is estimated for the five most active fields, along with the different volatility measures, and the results are presented in Tables 19-23. All fields are estimated to have an increasing hazard with p significantly greater than 1. In Prudhoe Bay, the log-likelihoods for models estimated using RV are generally higher than those estimated using any of the GARCH forecasts, whereas in the remaining fields the log-likelihoods for RV are generally smaller.

Duration Model III: Colville River

	RV	GARCH	GARCH-t	GARCH-GED	EGARCH	EGARCH-t	EGARCH-GED	GJR	GJR-t	GJR-GED
Vol	0.9994	0.9943*	0.9933	0.9940	0.9923	0.9940***	0.9915***	0.9947	0.9950	0.9937
	(0.0007)	(0.0034)	(0.0041)	(0.0037)	(0.0064)	(0.0015)	(0.0023)	(0.0039)	(0.0043)	(0.0050)
$RealOilPrice$	0.9317***	0.9182***	0.9155***	0.9169***	0.9315***	0.9261***	0.9206***	0.9169***	0.9196***	0.9121***
	(0.0185)	(0.0224)	(0.0247)	(0.0233)	(0.0121)	(0.0117)	(0.0143)	(0.0250)	(0.0252)	(0.0291)
$Tundra$	0.4844***	0.4757***	0.4798***	0.4797***	0.4742***	0.4398***	0.3947***	0.4857***	0.4930***	0.4959***
	(0.1137)	(0.1217)	(0.1181)	(0.1212)	(0.1076)	(0.1014)	(0.1346)	(0.1216)	(0.1174)	(0.1292)
$NumLeases$	0.9662***	0.9623***	0.9616***	0.9622***	0.9650***	0.9656***	0.9623***	0.9624***	0.9624***	0.9613***
	(0.0104)	(0.0101)	(0.0099)	(0.0102)	(0.0106)	(0.0111)	(0.0108)	(0.0111)	(0.0112)	(0.0113)
TVD	0.5992***	0.5846***	0.5811***	0.5820***	0.5036***	0.5575***	0.4645***	0.5833***	0.5816***	0.5784***
	(0.0392)	(0.0264)	(0.0229)	(0.0253)	(0.1032)	(0.0241)	(0.0500)	(0.0289)	(0.0272)	(0.0270)
$RigCount$	1.1354	1.1388	1.1385	1.1370	1.1605	1.1366	1.1565*	1.1379	1.1359	1.1392
	(0.1249)	(0.1086)	(0.1103)	(0.1866)	(0.1038)	(0.1097)	(0.0888)	(0.1101)	(0.1143)	(0.1098)
$SideTracks$	2.1170	2.1534	2.1423	2.1490	2.3961	2.2605	2.4949	2.1635	2.1361	2.1663
	(1.4759)	(1.4557)	(1.4499)	(1.4484)	(1.7543)	(1.5361)	(1.6972)	(1.4517)	(1.4630)	(1.4564)
Constant	3.1007	2.7574**	2.7636**	2.7837**	2.6085*	2.7474*	2.8680**	2.7942**	2.7664*	2.8447**
	(1.3530)	(0.8746)	(0.8786)	(0.8720)	(0.9146)	(0.9129)	(0.8511)	(0.8895)	(0.9193)	(0.8915)
p	1.63	1.76*	1.78*	1.77*	1.62**	1.66**	1.73***	1.77*	1.76*	1.83**
	(0.3951)	(0.4380)	(0.4422)	(0.4475)	(0.3165)	(0.3171)	(0.2403)	(0.4110)	(0.4023)	(0.4135)
LL	79.45	80.15	80.34	80.25	79.88	80.23	81.36	80.21	80.10	80.63

Table 19: Results for the duration model III for Colville River Field. Hazard ratios are reported; ***, **, and * denote hazard ratios that are different from one at the 1%, 5%, and 10%, respectively. Robust standard errors are in parenthesis. TVD: total vertical depth of the well in '000's of feet.

Duration Model III: Kuparuk River

	RV	GARCH	GARCH-t	GARCH-GED	EGARCH	EGARCH-t	EGARCH-GED	GJR	GJR-t	GJR-GED
Vol	0.9954***	0.9835***	0.9819***	0.9826***	0.9938	0.9878***	0.9878***	0.9843***	0.9835***	0.9839***
	(0.0016)	(0.0035)	(0.0038)	(0.0033)	(0.0050)	(0.0030)	(0.0030)	(0.0030)	(0.0033)	(0.0031)
$RealOilPrice$	0.9277***	0.9030***	0.8983***	0.9003***	0.9509***	0.9280***	0.9278***	0.9000***	0.9004***	0.8965***
	(0.0221)	(0.0177)	(0.0188)	(0.0171)	(0.0180)	(0.0193)	(0.0194)	(0.0200)	(0.0201)	(0.0202)
$Tundra$	0.8607	0.9107	0.9385	0.9261	0.8230	0.7690	0.7587	0.9387	0.9724	0.9455
	(0.1964)	(0.2023)	(0.2084)	(0.2047)	(0.1995)	(0.1690)	(0.1652)	(0.2055)	(0.2138)	(0.2062)
$NumLeases$	0.9517***	0.9493***	0.9485***	0.9490***	0.9617***	0.9625***	0.9624***	0.9419***	0.9482***	0.9492***
	(0.0071)	(0.0076)	(0.0079)	(0.0077)	(0.0077)	(0.0076)	(0.0076)	(0.0081)	(0.0078)	(0.0078)
TVD	0.5189***	0.5885***	0.5871***	0.5897***	0.5663***	0.5885***	0.5863***	0.5867***	0.5827***	0.5870***
	(0.1051)	(0.1102)	(0.1110)	(0.1109)	(0.1280)	(0.1292)	(0.1281)	(0.1073)	(0.1088)	(0.1065)
$RigCount$	1.1130*	1.0699	1.0620	1.0666	1.0839	1.0538	1.0542	1.0645	1.0573	1.0607
	(0.0614)	(0.0601)	(0.0612)	(0.0605)	(0.0626)	(0.0605)	(0.0605)	(0.0601)	(0.0614)	(0.0605)
$SideTracks$	1.7179	1.5408	1.5511	1.5509	1.4157	1.3303	1.3402	1.5791	1.6202	1.5694
	(0.5196)	(0.4604)	(0.4704)	(0.4724)	(0.4667)	(0.4599)	(0.4590)	(0.4693)	(0.5056)	(0.4603)
Constant	5.2725***	3.2544***	3.2618***	3.2627***	3.3762***	3.4954***	3.4933***	3.3036***	3.2780***	3.3507***
	(0.9699)	(0.5223)	(0.5422)	(0.5272)	(0.6072)	(0.5702)	(0.5720)	(0.5473)	(0.5661)	(0.5451)
p	2.46***	2.41***	2.42***	2.42***	2.22***	2.24***	2.24***	2.43***	2.45***	2.45***
	(0.2179)	(0.2280)	(0.2223)	(0.2251)	(0.2538)	(0.2394)	(0.2397)	(0.2328)	(0.2337)	(0.2350)
LL	399.65	403.62	406.97	406.69	369.16	387.99	388.65	407.90	410.33	411.17

Table 20: Results for the duration model III for Kuparuk River Field. Hazard ratios are reported; ***, **, and * denote hazard ratios that are different from one at the 1%, 5%, and 10%, respectively. Robust standard errors are in parenthesis. TVD: total vertical depth of the well in '000's of feet.

Duration Model III: Milne Point

	RV	GARCH	GARCH-t	GARCH-GED	EGARCH	EGARCH-t	EGARCH-GED	GJR	GJR-t	GJR-GED
Vol	0.9818	0.9651*	0.9581**	0.9641*	0.9750***	0.9826***	0.9825***	0.9710**	0.9665**	0.9697**
	(0.0115)	(0.0180)	(0.0198)	(0.0185)	(0.0028)	(0.0020)	(0.0020)	(0.0145)	(0.0167)	(0.0149)
$RealOilPrice$	0.8515*	0.8073**	0.7779***	0.7971**	0.8573***	0.8502***	0.8499***	0.7891**	0.7640**	0.7714***
	(0.0824)	(0.0755)	(0.0774)	(0.0824)	(0.0278)	(0.0295)	(0.0305)	(0.0850)	(0.0939)	(0.088)
$Tundra$	0.3302***	0.4574***	0.5785**	0.4555***	0.2915***	0.3440***	0.3435***	0.4546***	0.4868***	0.4807***
	(0.1057)	(0.1305)	(0.2150)	(0.1556)	(0.0961)	(0.1090)	(0.1106)	(0.1376)	(0.1815)	(0.1569)
$NumLeases$	0.9718	0.9353	0.9228	0.9354	1.0363*	1.0242	1.0238	0.9494	0.9424	0.9476
	(0.0288)	(0.0637)	(0.0676)	(0.0636)	(0.0203)	(0.0191)	(0.0187)	(0.0534)	(0.0586)	(0.0553)
TVD	0.5348***	0.7554	0.7959	0.7536	0.4738***	0.4762***	0.4780***	0.7443	0.7775	0.7718
	(0.1093)	(0.2091)	(0.2104)	(0.2005)	(0.0784)	(0.0736)	(0.0763)	(0.2050)	(0.2082)	(0.1999)
$RigCount$	1.3504**	1.3454**	1.3199**	1.4303***	1.2876**	1.3203**	1.3111**	1.3268**	1.3020**	1.3191**
	(0.1372)	(0.1423)	(0.1373)	(0.1423)	(0.1216)	(0.1400)	(0.1404)	(0.1388)	(0.1315)	(0.1415)
$SideTracks$	5.1458	5.4317*	5.7663***	5.8451**	8.4656***	8.0116***	8.0062***	5.1009*	5.7411***	4.7711**
	(3.2097)	(2.5032)	(1.7220)	(2.2979)	(2.5669)	(2.2663)	(2.2775)	(2.3558)	(1.6849)	(1.9028)
Constant	2.0738	3.7500***	3.7608***	3.8680***	5.5357***	5.5276***	5.5223***	4.2768***	4.3592***	4.3951***
	(1.0881)	(0.6529)	(0.6834)	(0.6393)	(0.7429)	(0.7333)	(0.7232)	(0.6012)	(0.6232)	(0.5902)
p	2.37*	2.89***	3.10***	2.98***	2.07***	2.12***	2.13***	2.95***	3.17***	3.09***
	(0.7189)	(0.3054)	(0.3596)	(0.3775)	(0.3377)	(0.3486)	(0.3367)	(0.2888)	(0.4560)	(0.3818)
LL	46.97	55.38	59.51	56.89	53.38	54.05	53.98	56.14	59.99	57.84

Table 21: Results for the duration model III for Milne Point Field. Hazard ratios are reported; ***, **, and * denote hazard ratios that are different from one at the 1%, 5%, and 10%, respectively. Robust standard errors are in parenthesis. TVD: total vertical depth of the well in '000's of feet.

Duration Model III: Nikaitchuq

	RV	GARCH	GARCH-t	GARCH-GED	EGARCH	EGARCH-t	EGARCH-GED	GJR	GJR-t	GJR-GED
Vol	1.0338***	1.1115***	1.1117***	1.1143***	1.0133	1.0622**	1.0678***	1.1162***	1.1159***	1.1207***
	(0.0088)	(0.0352)	(0.0350)	(0.0362)	(0.0137)	(0.0255)	(0.0310)	(0.0347)	(0.0345)	(0.0368)
$RealOilPrice$	0.9218***	1.0582*	1.0570*	1.0633*	0.8718*	0.8752**	0.9291**	1.1629**	1.1509**	1.1816**
	(0.0135)	(0.0344)	(0.0341)	(0.0365)	(0.0685)	(0.0636)	(0.0322)	(0.0665)	(0.0629)	(0.0742)
$Tundra$	2.0784**	1.5230*	1.5967**	1.4889*	3.3360	2.7530***	2.1776***	1.4976*	1.5827**	1.3925
	(0.4842)	(0.2711)	(0.2593)	(0.2751)	(1.4553)	(0.5011)	(0.0953)	(0.2955)	(0.2831)	(0.3098)
$NumLeases$	-	-	-	-	-	-	-	-	-	-
	-	-	-	-	-	-	-	-	-	-
TVD	0.1530***	0.1010***	0.1035***	0.1004***	0.2047***	0.0778***	0.0773***	0.1045***	0.1072***	0.1026***
	(0.0774)	(0.0815)	(0.0825)	(0.0807)	(0.2461)	(0.1024)	(0.0999)	(0.0864)	(0.0869)	(0.0860)
$RigCount$	0.8967	0.9095***	0.9114***	0.9095***	0.8236	0.7960	0.7925	0.9085***	0.9123***	0.9046***
	(0.0873)	(0.0340)	(0.0341)	(0.0331)	(0.1387)	(0.1397)	(0.1356)	(0.0276)	(0.0278)	(0.0263)
$SideTracks$	1.0947	1.4094	1.4160	1.4046	0.7632	0.7854	0.7536	1.4483	1.4643	1.4333
	(0.8658)	(1.0924)	(1.0933)	(1.0862)	(0.5778)	(0.5384)	(0.5287)	(1.0501)	(1.0581)	(1.0317)
Constant	2.6882***	5.8173***	5.8116***	5.8041***	6.2969***	7.2476***	7.0779***	5.6583***	5.6615***	5.6333***
	(0.2783)	(0.2436)	(0.2422)	(0.2353)	(1.1347)	(1.1325)	(1.0385)	(0.2293)	(0.2255)	(0.2189)
p	9.79 ***	14.03***	14.00***	14.26***	7.50***	8.01***	8.33***	14.57***	14.55***	15.03***
	(0.8395)	(1.9480)	(1.9367)	(2.0126)	(1.0686)	(0.9401)	(0.9543)	(1.9703)	(1.9711)	(2.1302)
LL	54.35	57.55	57.62	57.63	47.84	50.45	50.19	58.18	58.30	58.19

Table 22: Results for the duration model III for Nikaitchuq Field. Hazard ratios are reported; ***, **, and * denote hazard ratios that are different from one at the 1%, 5%, and 10%, respectively. Robust standard errors are in parenthesis. TVD: total vertical depth of the well in '000's of feet.

Duration Model III: Prudhoe Bay

	RV	GARCH	GARCH-t	GARCH-GED	EGARCH	EGARCH-t	EGARCH-GED	GJR	GJR-t	GJR-GED
Vol	0.9974***	0.9933***	0.9932***	0.9931***	0.9977	0.9964***	0.9964**	0.9931***	0.9931***	0.9930***
	(0.0004)	(0.0018)	(0.0018)	(0.0018)	(0.0023)	(0.0014)	(0.0014)	(0.0018)	(0.0017)	(0.0017)
$RealOilPrice$	0.9435***	0.9401***	0.9401***	0.9391***	0.9610***	0.9562***	0.9559***	0.9360***	0.9380***	0.9345***
	(0.0082)	(0.0095)	(0.0093)	(0.0096)	(0.0078)	(0.0084)	(0.0084)	(0.0100)	(0.0095)	(0.0101)
$Tundra$	0.5900***	0.5622***	0.5578***	0.5656***	0.5235***	0.5104***	0.5040***	0.5752***	0.5729***	0.5733***
	(0.0813)	(0.0781)	(0.0777)	(0.0777)	(0.0760)	(0.0737)	(0.0737)	(0.0799)	(0.0796)	(0.0794)
$NumLeases$	0.3440***	0.5062***	0.5109***	0.5020***	0.6638***	0.6509***	0.6341***	0.4917***	0.4886***	0.4862***
	(0.0580)	(0.1049)	(0.1054)	(0.1051)	(0.1110)	(0.1079)	(0.1079)	(0.1032)	(0.1041)	(0.1028)
TVD	0.6315***	0.6502***	0.6491***	0.6503***	0.6379***	0.6383***	0.6409***	0.6532***	0.6532***	0.6540***
	(0.0570)	(0.0640)	(0.0640)	(0.0636)	(0.0609)	(0.0601)	(0.0609)	(0.0655)	(0.0658)	(0.0657)
$RigCount$	1.0363	1.0208	1.0192	1.0193	1.0294	1.0252	1.0217*	1.0206	1.0174	1.0196
	(0.0342)	(0.0360)	(0.0361)	(0.0358)	(0.0375)	(0.0376)	(0.0372)	(0.0359)	(0.0359)	(0.0356)
$SideTracks$	2.8467**	2.4711**	2.4756**	2.4786**	2.3806**	2.3439**	2.3140**	2.4480**	2.4344**	2.4397**
	(0.7255)	(0.6239)	(0.6263)	(0.6273)	(0.6235)	(0.6040)	(0.6039)	(0.6230)	(0.6177)	(0.6182)
Constant	5.6394***	4.3215***	4.3248***	4.3356***	4.0644***	4.1183***	4.1419***	4.3684***	4.3537***	4.3931***
	(0.3208)	(0.2367)	(0.2370)	(0.2356)	(0.2600)	(0.2478)	(0.2458)	(0.2317)	(0.2287)	(0.2292)
p	2.06***	1.81***	1.81***	1.82***	1.63***	1.67***	1.68***	1.85***	1.85***	1.87***
	(0.1081)	(0.1472)	(0.1458)	(0.1502)	(0.1160)	(0.1179)	(0.1178)	(0.1536)	(0.1538)	(0.1568)
LL	613.15	569.91	569.73	570.78	556.75	559.58	560.47	572.58	572.81	574.14

Table 23: Results for the duration model III for Prudhoe Bay Field. Hazard ratios are reported; ***, **, and * denote hazard ratios that are different from one at the 1%, 5%, and 10%, respectively. Robust standard errors are in parenthesis. TVD: total vertical depth of the well in '000's of feet.

Whether using RV or one of the GARCH models as the volatility measure, the co-efficients remain close in magnitude within each individual field. Results for the largest and oldest field, Prudhoe Bay, are presented in Table 23. The effect of the volatility measure on the hazard rate of drilling varies the least among all of the fields: from 0.9930 to 0.9977. Results for the Kuparuk River field are presented in Table 20. Kuparuk River is another large, mature field, and the coefficients on the volatility measure vary from 0.9819 to 0.9954. In contrast, for the youngest field, Nikaitchuq (See Table 22), the co-efficients on the volatility measure vary the most: from 1.0133 to 1.1162. In Colville River (See Table 19), RV has the smallest effect on the hazard rate of drilling, relative to the other volatility measures, although RV coefficients for Colville River are almost all insignificant. The magnitudes on the coefficients for the various GARCH forecasts are all very close to 0.99 for most of the fields; Milne Point and Nikaitchuq have lower and higher magnitudes, respectively. Nikaitchuq is the only field where, regardless of the choice of volatility measure, the impact on the hazard rate is positive. Caution must be used when interpreting the results from Nikaitchuq since there are only 22 wells drilled during the sample period. Whether considering all of the fields pooled together, or each field individually, volatility is negatively related to the probability of drilling an oil well. These findings are consistent with Hurn and Wright (1994), and Dunne and Mu (2010), who also find a negative relationship between volatility and the hazard rate.

Interestingly, whereas the coefficients on the number of leases were insignificant when examining all of the fields pooled, when examining individual fields, they are significantly different from one at the 1% level in all of the fields except Milne Point - see Table 21. The Nikaitchuq field has 10 leases fixed for the sample period, thus the number of leases was not included in the regression. This suggests that overall, the effects from the number of leases a firm owns is not a significant factor in the hazard rate, but when disaggregating to the field level, the number of leases is important. The total vertical depth of a well has

varying effects on the hazard rate of drilling, mostly significant and negative, with Milne Point again the exception. That is, for most fields, the deeper the well, and thus the more expensive to drill, the lower the probability of drilling. While the effects vary from field to field, the coefficients are relatively insensitive to the choice of volatility measure. This is evident when pooling all of the fields or examining each field individually.

The hazard rate of drilling in Nikaitchuq also increases with a longer tundra season. A possible explanation for these effects is that Nikaitchuq is a relatively young field - production started in January 2011. For comparison, Prudhoe Bay has been in production since April, 1969. The number of drilling pads can also play a roll in the Nikaitchuq field since there are limited areas open to drilling and there are only 2 drilling pads. Only 22 wells were drilled in Nikaitchuq during the sample period, of which 8 are sidetracks. However, with the small sample size and a young field, caution must be used when drawing conclusions about the effects on the hazard rate of drilling in this field.

Insignificant when aggregating the fields in the simple model, the number of drilling rigs are also insignificant for the individual fields, with the exception of Milne Point. Kellogg (2011) notes that oil firms enter into long-term contracts with drilling firms, which could explain this finding. Another possible explanation is the limited number of drilling rigs and recent instances where demand exceeded supply (personal communication, manager with Nabor's Drilling Company, April 2012).

Prudhoe Bay and Milne Point, two of the oldest fields on the North Slope, are the only fields that show that side tracks are more likely to be drilled. Among the other fields, Kuparuk River is an interesting case. Of the 344 wells drilled during the sample period, 82% were sidetracks, whereas 88% of Prudhoe Bay's wells were side tracks. Kuparuk River and Prudhoe Bay have a similar number of drilling pad: 40 for the former and 44 for the latter; yet Prudhoe Bay drilled about 60% more wells. It is possible this difference could help explain why side tracks were not a significant factor in Kuparuk River, but it

is more likely due to unobserved factors specific to the individual fields.

As Prudhoe Bay ages, the producing gas to oil ratio increases, which occurs for two reasons. First, as the reservoir pressure drops, the ability of the oil to hold gas decreases and more free gas is released into the reservoir. Because gas flows through rock much more freely than liquids, the wells tend to start producing more gas and less liquids. Second, Prudhoe Bay has been using gas injection for enhanced oil recovery purposes for many years and the gas migrates from the injection wells to the producing wells, "pushing" oil as it goes. The sweep of gas through the reservoir is not 100% efficient, so there is still plenty of oil left to be produced. Over time the rate of oil production will decrease as the reservoir becomes more thoroughly swept. Eventually, the well will no longer be viable and it will be permanently shut, in pending abandonment or sidetracking to a new bottom hole location in the reservoir that hadn't previously been accessed. If the gas handling capacity at Prudhoe Bay was expanded, the point at which a well is permanently shut in would be delayed and there would not be as many side tracks needed. A large percentage of wells in Prudhoe Bay have been sidetracked, with some being sidetracked 5 or more times in the field's 35 years of production. Thus, facility constraints are not a constraint to new drilling activity and actually encourage new drilling. Therefore, decisions to drill new oil wells are mainly governed by the capacity of the gas handling plants, not pricing variables.

Given that the largest field on the North Slope is gas limited, the results presented here show that oil drilling is not very responsive to oil price volatility. Perhaps the gas limited nature of the Prudhoe Bay field leads to more drilling in response to higher oil prices because side track wells are relatively cheaper to drill and permit the firms to access smaller pools of oil that are otherwise unprofitable. This also helps to explain the results seen in Nikaitchuq - specifically the response to volatility and the generally lower probability of drilling a side track - since the field is younger and not yet constrained by

the same physical characteristics of the larger, more mature Prudhoe Bay field. To put this into context of this study, the gas limited nature of Prudhoe Bay encourages side track drilling to reach pockets of oil left after the enhanced oil recovery effort. Side tracks are more likely to be drilled in the mature fields - specifically Prudhoe Bay.

Conclusion

The objective of this chapter is to perform an empirical study of how firms on the North Slope of Alaska behave in response to oil price volatility, using real options theory and a parametric proportional hazard model. I find the hazard of drilling is increasing with time both in aggregate and at the field level. Furthermore, in aggregate, an increase in uncertainty, measured by monthly GARCH forecasts or realized volatility, decreases the hazard rate of undertaking the irreversible investment of drilling an oil well. These results are robust to the choice of volatility measure. When choosing a GARCH (1,1), EGARCH (1,1), or GJR-GARCH (1,1) forecast as the volatility measure, the response to an increase in uncertainty is a decrease in the hazard rate of magnitude similar to that when RV is chosen: about a 0.16% to 0.8% decrease for every one unit increase in volatility. Field specific effects of volatility vary in magnitude, however, most fields show a negative relationship between oil price volatility and oil well drilling, with only the relatively young Nikaitchuq field exhibiting a positive relationship between the hazard rate and oil price volatility.

The expected impact of an increase in real oil prices is that firms would increase their investment, or drill more wells. In this study, the opposite is seen. One explanation for these results is that the gas limited nature of Prudhoe Bay presents a non-economic constraint to firms' operations and thus, firms are not as responsive to oil price or oil price volatility as they are to operating capacity. It is also possible that relatively short-term measures such as monthly oil price volatility or monthly oil price, are not completely relevant to firms' long-term investment decisions (Favero, Pesaran, and Sharma, 1994). This

highlights the need for a better understanding of how firms respond to long-term volatility and price trends. Future work will investigate both firms' response to longer-term economic variable measures and also analyze production responses to changing volatility. One challenging aspect to this line of research is the incidental truncation issue inherent with the decision to drill. If higher volatility leads to a delay in oil drilling, then it is also possible that some wells are not drilled. Not including a correction for this incidental truncation when modeling the response of production to volatility could lead to sample selection bias.

REFERENCES

1. Abosedra, S. S. and N. T. Laopodis (1997), "Stochastic behavior of crude oil prices: a GARCH investigation," *Journal of Energy and Development*, 21:2, 283-291.

2. Alaska Department of Natural Resources, Division of Mining, Land, and Water (2015), "Fact Sheet: Off-Road Travel on the North Slope on State Land,"Retrieved from `http://dnr.alaska.gov/mlw/factsht/land_fs/off-road_travel.pdf`

3. Alaska Oil and Gas Conservation Commission (AOGCC), 2014, Oil and Gas Data Web Application. Available at: `http://doa.alaska.gov/ogc/publicdb.html`. Accessed July 2015.

4. Alquist, R., and L. Kilian (2010), "What do we learn from the price of crude oil futures?," *Journal of Applied Econometrics*, 25:4, 539-573.

5. Alquist, R., L. Kilian and R. J. Vigfusson (2013), "Forecasting the Price of Oil," in: G. Elliott and A. Timmermann (eds.), *Handbook of Economic Forecasting*, 2, Amsterdam: North-Holland: 427-507.

6. Andersen, T. G. and T. Bollerslev (1998), "Answering the Critics: Yes ARCH Models Do Provide Good Volatility Forecasts,"*International Economic Review*, 39:4, 885-905.

7. Andersen, T. G., T. Bollerslev, P. F. Christoffersen and F. X. Diebold (2006), "Volatility and Correlation Forecasting," Handbook of Economic Forecasting, Amsterdam: North-Holland, 778-878.

8. Andersen, T. G., T. Bollerslev, F. X. Diebold, and P. Labys (2003), "Modeling and forecasting realized volatility,"*Econometrica*, 71:2, 579-625.

9. Arrow, K. J. (1968), "Optimal Capital Policy with Irreversible Investment,"in *Value, Capital and Growth, Essays in Honor of Sir John Hicks,* ed. James N. Wolfe. Edinburgh, Scotland: Edinburgh University Press.

10. Bernanke, B. (1983), "Irreversibility, Uncertainty, and Cyclical Investment," *The*

Quarterly Journal of Economics, 98:1, 85-106.

11. Bigsten, A., P. Collier, S. Dercon, M. Fafchamps, B. Gauthier, J. W. Gunning, R. Oostendorp, C. Patillo, M. Söderbom, and F. Teal (2005), "Adjustment Costs and Irreversibility as Determinants of Investment: Evidence from African Manufacturing," *Contributions to Economic Analysis and Policy,* 4:1.

12. Bina, C., and M. Vo (2007) "OPEC in the epoch of globalization: an event study of global oil prices," *Global Economy Journal*, 7:1.

13. Blair, B. J., S. Poon, and S. Taylor (2001), "Forecasting S&P 100 volatility: the incremental information content of implied volatilities and high-frequency index returns," *Journal of Econometrics*, 105, 5-26.

14. Bollerslev, T. (1986), "Generalized Autoregressive Conditional Heteroskedasticity," *Journal of Econometrics*, Vol 31, No 3, 307-327.

15. Bollerslev, T., R. F. Engle, and D. B. Nelson (1994) "ARCH models," Handbook of econometrics 4: 2959-3038.

16. Boyce, J. R. and L. Nøstbakken (2011), "Exploration and development of U.S. oil and gas fields,1955-2002," *Journal of Economics Dynamics and Control*, 35, 891-908.

17. Bulan, L., C. Mayer, and C. T. Somerville (2009), "Irreversible investment, real options, and competition: Evidence from real estate development," *Journal of Urban Economics*, 65, 237-251.

18. Caporale, G, N. Pittis and N. Spagnolo (2003), "IGARCH models and structural breaks," *Applied Economics Letters*, Vol 10, No 12, 765-768.

19. Carrasco, M, L. Hu and W. Ploberger (2014), "Optimal Test for Markov Switching Parameters," *Econometrica*, Vol 82, No 2, 765-784.

20. Davis, L.W., Kilian, L. (2011) "The allocative cost of price ceilings in the US residential market for natural gas," *Journal of Political Economy* 119, 212–241.

21. Diebold, F. X. and R. S. Mariano (1995), "Comparing Predictive Accuracy," *Journal*

of Business and Economic Statistics, 13:3, 253-263.

22. Dixit, A. K., and R. S. Pindyck (1994), "Investment Under Uncertainty,"Princeton, NJ: Princeton University Press.

23. Dunne, T. and X. Mu (2010), "Investment Spikes and Uncertainty in the Petroleum Refining Industry,"*Journal of Industrial Economics*, 58, 190-213.

24. Engle, R. F. (1982), "Autoregressive Conditional Heteroskedasticity with Estimates of U.K. Inflation,"*Econometrica,* 50:4, 987-1008.

25. Favero, C.A., M. H. Pesaran, and S. Sharma (1994), "A Duration Model of Irreversible Oil Investment: Theory and Empirical Evidence," *Journal of Applied Econometrics*, 9, S95-S112.

26. Ferderer, J. P. (1996), "Oil price volatility and the macroeconomy,"*Journal of Macroeconomics,* 18:1, 1-26.

27. Fong, W., and K. See (2002), "A Markov switching model of the conditional volatility of crude oil futures prices," *Energy Economics*, 24, 71-95.

28. Gantt, L. L., E. Oba, M., L. Leising, T. Stagg, M. Stanley, E. Walker, and R Walker (1998), "Coiled tubing drilling on the Alaskan North Slope,"*Oilfield review*, 10:2, 20-35.

29. Garcia, R. (1998),"Asymptotic Null Distribution of the Likelihood Ratio Test in Markov Switching Models,"*International Economic Review*, 39, 763-788.

30. Ghysels, E., A. Rubia, and R. Valkanov (2009), "Multi-Period Forecasts of Volatility: Direct, Iterated, and Mixed-Data Approaches," working paper, University of North Carolina.

31. Ghysels, E., P. Santa-Clara, and R. Valkanov (2005), "There is a Risk-Return Trade-off After All," *Journal of Financial Economics*, 76, 509–548.

32. Ghysels, E., P. Santa-Clara, and R. Valkanov (2006), "Predicting volatility: getting the most out of return data sampled at different frequencies," *Journal of Economet-*

rics, 131, 59–95.

33. Giacomini, R. and H. White (2006), "Tests of Conditional Predictive Ability," *Econometrica*, 74, 1545-1578.

34. Glosten, L., R. Jagannathan and D. Runkle (1993), "On the Relation Between Expected Value and the Volatility of Nominal Excess Returns on Stocks," *Journal of Finance,* 48, 1779-1901.

35. Gray, S. (1996), "Modeling the Conditional Distribution of Interest Rates as a Regime-Switching Process," *Journal of Financial Economics,* 42, 27-62.

36. Haas, M., S. Mittnik and M. Paolella (2004), "A New Approach to Markov Switching GARCH Models," *Journal of Financial Econometrics*, 2, 493-530.

37. Hansen, B. (1992), "The Likelihood Ratio Test Under Non-Standard Conditions: Testing the Markov Switching Model of GNP," *Journal of Applied Econometrics*, 7, S61-S82.

38. Hansen, P. R. (2005), "A Test for Superior Predictive Ability," *Journal of Business and Economic Statistics,* 23:4, 365-380.

39. Hansen, P. R. and A. Lunde (2005), "A forecast comparison of volatility models: Does anything beat a GARCH(1,1)?," *Journal of Applied Econometrics*, 20, 873-889.

40. Hou, A, and S. Suardi (2012) "A nonparametric GARCH model of crude oil price return volatility," *Energy Economics*, 34, 618-626.

41. Hurn, A. S. and R. E. Wright (1994), "Geology or Economics? Testing Models of Irreversible Investment Using North Sea Oil Data," *Economic Journal*, 104, 363-371.

42. Kahn, J.A. (1986) "Gasoline prices and the used automobile market: a rational expectations asset price approach," *Quarterly Journal of Economics* 101, 323–340.

43. Kellogg, R. S. (2011), "Learning by Drilling: Interfirm Learning and Relationship Persistence in the Texas Oilpatch," *Quarterly Journal of Economics,* 104, 1698-1734.

44. Kellogg, R. S. (2014), "Irreversibility, Uncertainty, and Investment," *American Economic Review,* 126, 1961-2004.

45. Kiefer, N. M. (1988), "Economic Duration Data and Hazard Functions," *Journal of Economic Literature,* 26, 646-679.

46. Klaassen, F. (2002), "Improving GARCH Volatility Forecasts," *Empirical Economics,* 27:2, 363–94

47. Lamoureux, C. G., and W. D. Lastrapes (1990), "Persistence in variance, structural change, and the GARCH model," *Journal of Business and Economic Statistics*, 8.2, 225-234.

48. Leighty, W. and C. -Y. Cynthia Lin (2012), "Tax policy can change the production path: A model of optimal oil extraction in Alaska," *Energy Policy,* 41, 759-774.

49. Liu, L, A. J. Patton and K. Sheppard (2012), "Does anything beat 5-minute RV? A comparison of realized measures across multiple asset classes," Duke University, Working Paper.

50. Lopez, J. A. (2001), "Evaluating the Predictive Accuracy of Volatility Models," *Journal of Forecasting,* 20:2, 87-109.

51. Marcucci, J. (2005), "Forecasting Stock Market Volatility with Regime-Switching GARCH Models," *Studies in Nonlinear Dynamics and Econometrics*, Vol. 9, Issue 4, Article 6.

52. Marschak, J. (1949), "Rule of liquidity under complete and incomplete information," *The American Economic Review Papers and Proceedings,* 39:3, 182-195. *Review of Financial Studies*, 15, 370-379.

53. Moel, A. and P. Tufano (2002), "When are Real Options Exercised? An Empirical Study of Mine Closings," *The Review of Financial Studies,* 15, 35-64.

54. Mohammadi, H., and L. Su (2010) "International evidence on crude oil price dynamics: Applications of ARIMA-GARCH models ," *Energy Economics*, 32, 1001-1008.

55. Morana, C. (2001), "A semi-parametric approach to short-term oil price forecasting," *Energy Economics*, Vol 23, No 3, 325-338.

56. Nelson, D. B. (1990), "Stationarity and Persistence in the GARCH(1,1) Model," *Econometric Theory*, 6:3, 318-334.

57. Nelson, D. B. (1991), "Conditional Heteroskedasticity in Asset Returns: A New Approach," *Econometrica*, 59:2, 347-370.

58. Nomikos, N., and P. Pouliasis (2011), "Forecasting petroleum futures markets volatility: The role of regimes and market conditions," *Energy Economics*, 33, 321-337.

59. Pagan, A. R., and G. W. Schwert (1990), "Alternative models for conditional stock volatility," *Journal of Econometrics,* 45:1, 267-290.

60. Pesaran, M. H. and A. Timmermann (1992), "A Simple Nonparametric Test of Predictive Performance," *Journal of Business and Economic Statistics*, 10:4, 461-465.

61. Pindyck, R. (1991), "Irreversibility, Uncertainty, and Investment," *Journal of Economic Literature,* 29:3, 1110-1148.

62. Plante, M., and N. Traum, (2012). Time-varying oil price volatility and macroeconomic aggregates. Center for Applied Economics and Policy Research Working Paper, (2012-002).

63. Politis, D. N. and J.P. Romano (1994), "The Stationary Bootstrap," *Journal of The American Statistical Association*, 89:428, 1303-1313.

64. U.S. Department of Energy, National Energy Technology Laboratory (2005), "Alaska Coiled Tubing: State of the Industry and Role for NETL,"(Report No DE-AD26-00NT00612), Retrieved from `http://www.netl.doe.gov/kmd/cds/disk17/C%20-%20Drilling%20Completion%20Stimulation/NT00612-Coiled%20Tubing.pdf`.

65. Vo, M. (2009), "Regime-switching stochastic volatility: Evidence from the crude oil market," *Energy Economics*, 31, 779-788.

66. West, K. D. (1996), "Asymptotic Inference About Predictive Ability," *Econometrica*, 64, 1067-1084.

67. White, H. (2000), "A Reality Check for Data Snooping," *Econometrica*, 68:5, 1097-1126.

68. Wilson, B., R. Aggarwal and C. Inclan (1996), "Detecting volatility changes across the oil sector," *Journal of Futures Markets*, 47:1, 313-320.

69. Xu, B. and J. Oueniche (2012), "A Data Envelopment Analysis-Based Framework for the Relative Performance Evaluation of Competing Crude Oil Prices' Volatility Forecasting Models," *Energy Economics*, 34:2 576-583.

ABSTRACT

ESSAYS ON OIL PRICE VOLATILITY AND IRREVERSIBLE INVESTMENT

by

DANIEL J. PASTOR

May 2016

Advisor: Dr. Robert Rossana

Major: Economics

Degree: Doctor of Philosophy

In chapter 1, we provide an extensive and systematic evaluation of the relative forecasting performance of several models for the volatility of daily spot crude oil prices. Empirical research over the past decades has uncovered significant gains in forecasting performance of Markov Switching GARCH models over GARCH models for the volatility of financial assets and crude oil futures. We find that, for spot oil price returns, non-switching models perform better in the short run, whereas switching models tend to do better at longer horizons.

In chapter 2, I investigate the impact of volatility on firms' irreversible investment decisions using real options theory. Cost incurred in oil drilling is considered sunk cost, thus irreversible. I collect detailed data on onshore, development oil well drilling on the North Slope of Alaska from 2003 to 2014. Volatility is modeled by constructing GARCH, EGARCH, and GJR-GARCH forecasts based on monthly real oil prices, and realized volatility from 5-minute intraday returns of oil futures prices. Using a duration model, I show that oil price volatility generally has a negative relationship with the hazard rate of drilling an oil well both when aggregating all the fields, and in individual fields.

AUTOBIOGRAPHICAL STATEMENT

Daniel J. Pastor grew up in suburban Metro Detroit and earned a Bachelor's of Science cum laude in Mathematics from Wayne State University in 2007. He went on to earn a Masters degree in Economics and completed his PhD in Economics in 2016. When not working, he likes to enjoy all types of outdoor activities.